McGill University

Early pro-atherogenic changes induced by vaping in a mouse model

By: Bayan Ibrahim Alakhtar, PharmD

Faculty of Medicine and Health Sciences

Department of Experimental Medicine

McGill University, Montreal

A thesis submitted to McGill University in partial fulfillment of the requirements of the of Master of Science

Table of Contents

List of figures

List of tables

Abbreviations

COPD: chronic obstructive pulmonary disease.

IQOS: heat-not-burn products.

e-cigarettes: electronic cigarettes.

PG: propylene glycol.

VG: vegetable glycerin.

$t_{1/2}$: half life.

Ni: nickel.

Cr: chromium.

EVALI: vaping use-associated lung injury.

BAL: bronchoalveolar lavage.

LPS: lipopolysaccharide.

CVD: cardiovascular diseases.

IHD: ischemic heart disease.

MI: myocardial infarction.

AMI: acute myocardial infarct.

LDL: low-density lipoprotein.

HDL: high density lipoprotein.

SMC: smooth muscle cells.

EC: endothelial cell.

WBCs: white blood cells.

ROS: reactive oxygen species.

MMPs: Matrix metalloproteinase.

IL: interleukin.

ICAM-1: intracellular cell adhesion molecule-1

VCAM-1: vascular cell adhesion molecule-1

DCs: dendritic cells.

VSMCs: vascular smooth muscle cells.

TNF-α: tumour necrosis factor alfa.

VECs: vascular endothelial cells.

IgSF: immunoglobulin superfamily.

PECAM-1: platelet endothelial cell adhesion molecule.

E-selectin: endothelium-selectin.

P-selectin: platelet-selectin.

L-selectin: leukocyte selectin.

PSGL-1: p-selectin glycoproteinligand-1.

VLA-4: Very late antigen-4.

LFA-1: lymphocyte function-associated antigen-1.

IFN-γ: interferon-gamma.

PAMPs: pathogen-associated molecular complexes.

APCs: antigen-presenting cells.

MHC: major histocompatibility complex.

TCR: T cell receptor.

Th: helper T.

Tregs: regulatory T cells.

CCR: chemokine receptor.

$Apoe^{-/-}$: apolipoprotein E knockout mice.

$LDLr^{-/-}$: low density lipoprotein receptor deficient mice.

PCSK9: protein convertase subtilisin/kexin type 9.

BBB: blood–brain barriers.

AD: Alzheimer disease.

rAAV: recombinant adeno-associated virus.

PGE2: prostaglandin E2.

8-OHdG: 8-hydroxy-2'-deoxyguanosine.

MDA: malondialdehyde.

IHC: immunohistochemistry.

BCA: brachiocephalic artery.

FMO: fluorophore-minus-one.

PPARs: peroxisome proliferator-activated receptors.

Acknowledgement

First and foremost, I would like to express my sincere thanks and appreciation to my supervisor ,Dr.Koren Mann, Division pf pharmacology and therapeutic at McGill university, for her invaluable assistance and support during this project. Her aid and devotion have been unwavering, and this paper would not have been accomplished without her. Her consistent and outstanding mentorship is much valued.

Many thanks to my past and present colleagues in the laboratory who shared
their technical experience and support, particularly those who contributed to my project, Kiran Makhani, Nivetha Subramaniam, Terek been, Braden Gill, Rowa Bakadlag, Sara Ghandour and our lab manger Cynthia Guilbert. I have completely valued your input throughout this whole process.

I would like to thank my friend Donna Patterson, whose guidance and unlimiting support and care have not gone unnoticed and are very much appreciated.

Finally, I am forever indebted to my loving parents Ibrahim and Moudy, my sisters and brother for their constant support, inspiration, and encouragement during my years of study.

Also, to my husband Ali and to my daughters Aljawharah and Adeem for their understanding, patience, and unconditional support. This accomplishment would not have been achievable without them. Thank you.

Contribution of authors

Bayan Alakhtar: designed the experiment, performed the experiment, analyzed the data, and wrote the thesis.

Koren Mann: supervised the study, provided the infrastructure, designed the experiment, reviewed the data analysis, and reviewed the thesis.

Carolyn Baglole: provided the infrastructure and designed the experiment.

Terek Been: designed the experiment, conducted the mice exposure, and helped with harvesting the organs.

Kiran Makhani and Nivetha Subramaniam: helped with harvesting the organs.

Cynthia Guilbert: performed the western blot experiment.

Conflict of interest

No conflicts of interest, financial or otherwise, are declared by the authors.

Abstract

JUUL is a brand of e-cigarette popular with both smokers and those who have never smoked, including teenagers. Despite the widespread use of JUUL and the anticipated negative cardiovascular effects of nicotine, no data exist on the impact of JUUL vaping on the development of atherosclerosis. The aim of this study was to evaluate whether exposure to JUUL e-cigarette aerosols induced early pro-atherogenic alterations in young murine atherosclerotic models. To do so, the effects of vaping mango-flavored JUUL aerosols was compared to room air and vehicle (polyethylene glycol: vegetable glycerin; PG/VG) in an inducible murine model of atherosclerosis. Here, adeno-associated viral particles containing the human protein convertase subtilisin/kexin type 9 (PCSK9) variant were injected in male C57BL/6J mice to promote degradation of the low-density lipoprotein receptor in the liver, resulting in hyperlipidemia and atherosclerosis in mice. Mice were fed a high-fat diet and exposed to room air or commercially-available JUUL pods containing only PG/VG or 5% nicotine with mango flavor at a rate of 4 puffs/min, 3 times a day for 4 weeks, an exposure scenario that mimics human cotinine levels in moderate users. Early vascular toxicities were evaluated including pro-atherogenic circulatory markers and atherosclerotic plaque. In addition, immune outcomes were examined including changes in lymphoid and myeloid cells composition. Our results showed that exposure to either PG/VG or mango-flavored JUUL prevented mice from gaining weight. Although quite early in atherogenesis, PG/VG-containing JUUL trended towards increased plaque size, although this was not observed with mango-flavored JUUL. In contrast, mango-flavored JUUL, but not air or PG/VG, decreased circulating HDL and glucose levels. Finally, immunophenotyping of the spleen following inhalation of JUUL aerosols showed that mango-flavored JUUL decreased CD4+ T cells, while PG/VG tended towards increased CD8+ T cells, although the latter wasn't significant. These results demonstrate that JUUL exposure can induce early pro-atherogenic alterations in young hyperlipidemic mice, suggesting there could be increased cardiovascular disease later in life.

Résumé

JUUL est une marque de cigarette électronique populaire auprès des fumeurs et de ceux qui n'ont jamais fumé, y compris les adolescents. Malgré l'utilisation généralisée de JUUL et les effets cardiovasculaires négatifs anticipés de la nicotine, aucune donnée n'existe sur l'impact du vapotage JUUL sur le développement de l'athérosclérose. L'objectif de cette étude était d'évaluer si l'exposition aux aérosols de cigarettes électroniques JUUL induitdes altérations pro-athérogènes précoces dans de jeunes modèles athérosclérotiques murins. Pour ce faire, les effets du vapotage d'aérosols JUUL aromatisés à la mangue ont été comparés à l'air ambiant et au véhicule (polyéthylène glycol: glycérine végétale; PG/VG) dans un modèle murin inductible d'athérosclérose. Ici, des particules virales adéno-associées contenant l'humain (protéine convertase subtilisine/kexine de type 9; PCSK9) ont été injectés chez des souris mâles C57BL/6J pour favoriser la dégradation du récepteur des lipoprotéines de basse densité dans le foie, entraînant une hyperlipidémie et une athérosclérose chez la souris. Les souris ont été nourries avec un régime riche en graisses et exposées à l'air ambiant ou à des gousses JUUL disponibles dans le commerce contenant uniquement du PG / VG ou 5% de nicotine avec une saveur de mangue à raison de 4 bouffées / min, 3 fois par jour pendant 4 semaines, un scénario d'exposition qui imite les niveaux de cotinine humaine chez les utilisateurs modérés. Les toxicités vasculaires précoces ont été évaluées, y compris les marqueurs circulatoires pro-athérogènes et la plaque athéroscléreuse. En outre, les résultats immunitaires ont été examinés, y compris les changements dans la composition des cellules lymphoïdes et myéloïdes. Nos résultats ont montré que l'exposition à JUUL empêchait les souris de prendre du poids. De plus, après quatre semaines d'exposition et un régime riche en graisses, JUUL a entraîné une tendance à l'augmentation des résultats athérosclérotiques de manière indépendante de la nicotine. Ceci, accompagné de JUUL, a entraîné une diminution des niveaux de HDL et de glucose. Enfin, l'inhalation d'aérosols JUUL a augmenté les indices d'inflammation systémique modélisés par une diminution des CD4 et une augmentation des CD8 dans la rate. Ces résultats démontrent que l'exposition à JUUL peut induire des altérations pro-athérogènes précoces chez les jeunes souris hyperlipidémiques, suggérant qu'il pourrait y avoir une augmentation des maladies cardiovasculaires plus tard dans la vie.

Chapter One: Introduction and background

1. Electronic Cigarette- overview

1.1 Historical context of electronic cigarette use

Tobacco smoking remains the leading cause of preventable death worldwide (1). Its considered one of the greatest risk factors in developing chronic diseases, such as chronic obstructive pulmonary disease (COPD) and lung cancer (1). As people became more attentive to the negative health effects of tobacco use, the concept of developing a technique mimicking smoking emerged. As such, about a decade ago, the employment of emerging nicotine-based products, such as heat-not-burn products (IQOS) and electronic cigarettes (e-cigarettes), increased among smokers worldwide (1, 2). E-cigarettes initially hit the market in the United States in 2006 and were designed to mimic the act of smoking but limit tobacco consumption and combustion, which is associated with carcinogen release (3). This feature contributed to their gain in popularity as a smoking cessation tool and an improved alternative to conventional cigarettes (4). In fact, in keeping with multiple surveys, the bulk of e-cigarette users feel that not only are e-cigarettes less dangerous than regular tobacco cigarettes, but that these devices may additionally help people quit smoking traditional cigarettes (5, 6). The literature shows that while e-cigarettes may be effective smoking cessation aids, abstinence rates are significantly lower than those seen in studies employing traditional smoking cessation methods (7).

E-cigarettes have developed from early generation cigarette look-a-likes (cigalikes), to customizable tank-style e-cigarettes, to the latest, more unobtrusive gadget type known as pod mods or "pods". JUUL is the most well-known pod mod, initially being introduced in 2015 (4). In 2019, JUUL was the most popular brand of e-cigarette in North America, accounting for over 70% of the US and Canadian e-cigarette market (8, 9). Its sleek design, user-friendly function,

desirable flavors, and ability to be used discreetly in places where smoking is forbidden are all appealing features resulting in JUUL gaining popularity among adolescents and young adults (4). The results of a survey done in 2017 found that 19% of individuals aged 15-24 were regular JUUL users (10). Moreover, according to the American National Youth Tobacco Survey done in 2019, 27.5% of high school students and 10.5 % of middle school students were current users of e-cigarettes (defined as usage in the last 30 days) (7, 11). Despite the dramatic increase in e-cigarette use among teens and young adults in the US and Canada (2), the health effects of e-cigarette use among never-smokers continues to be largely unknown.

1.2 Electronic cigarette components

Currently, there are more than 460 e-cigarette brands with more than 8000 unique e-liquid flavors available on the market (12). The basic components of these e-cigarette brands include the rechargeable battery, the atomizer (or heating element/coil) and the liquid cartridge that holds the e-liquid. E-liquids contain a solvent (usually propylene glycol [PG] and vegetable glycerin [VG]), nicotine and various additives including flavors (7). When an e-cigarette user takes a puff via the mouthpiece, an air-flow sensor is activated, allowing the atomizer to heat the e-liquid and generate an aerosol for inhalation into the lungs (7). As previously mentioned, JUUL is a pod style e-cigarette, and one pod contains the same amount of nicotine as two packs of cigarettes (13). JUUL e-liquids contain a nicotine base and a weak organic acid (*e.g.*, benzoic acid) that forms a nicotine salt, which is more tolerable to the lungs when inhaled resulting in delivery of higher amount of nicotine into the lungs when compared to previous free-base nicotine (14, 15). Nicotine and its primary metabolite cotinine are widely utilized as objective biomarkers of exposure, with cotinine being preferred due to its longer half-life in vivo ($t_{1/2}$ = 2 hours for nicotine vs 16-18 hours for cotinine in humans)(16). CYP2A5, a mouse cytochrome

P450 monooxygenase that shows high similarity to human CYP2A6, is responsible for metabolizing nicotine into cotinine (17). For e-cigarette users, cotinine levels can range from 13.9-300 ng/mL (18, 19). Mango, mint, and tobacco flavors are among the most popular flavors in JUUL pods (20).

E-liquids also contain traces of many inorganic elements and toxic metals, such as sodium, bromine, gold, scandium, iron, and cobalt (7). Moreover, in JUUL e-cigarettes, the heating coil is usually made of nichrome (a combination of nickel (Ni) and chromium (Cr)) and stainless steel). Toxic metals from heated coils can leach into the e-liquids then into vaping aerosols (7). A study published in 2017 sought to determine if e-cigarette usage related to increased Ni and Cr exposure (21). In the study, they measured Ni and Cr levels in urine, saliva, and exhaled breath condensate (as non-invasive biomarkers) from 64 e-cigarette users. They found positive correlations between Ni and Cr aerosol concentrations found in the aerosol with Ni and Cr concentrations found in the tested biomarkers, indication that e-cigarette emissions enhance metal internal dosage. Furthermore, they found that greater e-cigarette usage and consumption are associated with higher Ni biomarker levels. Additionally, another study published in 2018 sought to determine if metals from the heating coil leach into the e-liquid in the e-cigarette tank and the generated aerosol (22). In the study, they assessed the concentration of metals, such as Ni and Cr, in samples collected from the refilling dispenser, aerosol, and leftover e-liquid in the tank using 56 e-cigarette devices from daily e-cigarette users. They discovered remarkable increases in metal concentrations in the aerosol and tank samples compared to the refilling dispenser (22). Their findings revealed that coil contact caused e-liquid contamination, implying that e-cigarettes are a possible source of harmful metal exposure such as Cr and Ni (22).

As such, utilizing both e-cigarette devices and its e-liquid at the same time in investigations is of a great value in understanding their aggregate adverse effects. In addition, while many of the components in e-liquids are 'Generally Recognized as Safe' for oral consumption, there is limited information on their safety when aerosolized and inhaled (23).

1.3 Health impact of electronic cigarettes

The widespread usage of e-cigarettes among non-smokers and teens raised concerns over the health effects from vaping. While statistics on the health effects of traditional tobacco are vast, research on e-cigarettes and vaping devices is less established. The assessment of the health impact of vaping is challenged by the existence of 460 e-cigarette brands with over 8000 distinct e-liquid flavors along with the rapid evolution of vaping devices (12).

The emergence of a serious lung condition known as e-cigarette or vaping use-associated lung injury, “EVALI”, or “vape lung” has piqued the interest of scientists. EVALI has been linked to symptoms such as shortness of breath, coughing, and hypoxemia (24). In addition, lipid-laden macrophages were found present in bronchoalveolar lavage (BAL) of many patients diagnosed with EVALI (25). Interestingly, lipid-laden macrophages are also a major feature in atherosclerosis, which is a chronic inflammatory response in the walls of arteries characterised by macrophage accumulation (the pathogenesis of atherosclerosis will be discussed in detail in section 2.2) (26). As a result, it cannot be ruled out that EVALI patients are more prone to developing atherosclerosis. Furthermore, the most likely causative factor for EVALI is currently assumed to be vitamin E acetate, which is utilised as a thickening ingredient in counterfeit THC-containing goods in the United States (27). Although, JUUL products do not include vitamin E acetate, there is limited information on their safety when aerosolized and inhaled (23).

The exposure to currently available JUUL flavored pods negatively impacts health in a flavour-dependent manner. The bulk of current research on the cytotoxic effects of various JUUL flavours (creme brulee, cool mint, fruit medley, tobacco, menthol, etc.) on respiratory system cells, conducted *in vitro*, indicate that JUUL aerosols are cytotoxic and impede cell function, the significance of which is dependent on the flavour used (12, 15, 28-33). Furthermore, in a study conducted by our group, we sought to assess acute exposure (3-days) to JUUL e-cigarette aerosols in three popular flavours (mint, tobacco, and mango) using a mouse model (34). According to our findings, even short-term inhalation of flavoured JUUL e-cigarette aerosols promoted differential immunological regulation and oxidative stress responses. Moreover, flavours were found to differentially impact the extent of these modulations (34).

Research also looked at the effects of chronic aerosol inhalation on cardiopulmonary function and inflammation across organ systems using the JUUL device. In the study, female mice were placed in individual sections of a full-body exposure chamber, where they were exposed to either mint or mango flavoured aerosols daily for either four weeks or three months to assess the effect of JUUL on the brain, lung, heart, and colon (35). According to the findings, chronic JUUL inhalation is associated with neuroinflammation in the brain, alters inflammatory- and fibrosis-associated gene expression in cardiac tissue, and alters pro-inflammatory markers in the colon (35). On the other hand, the study also found that daily JUUL aerosol inhalation does not alter heart rate and blood pressure or alter pulmonary physiology (35). Additionally, chronic JUUL inhalation does not change the inflammatory state of lungs under both homeostatic and lipopolysaccharide (LPS) challenge conditions, and does not induce cardiac, renal or liver fibrosis (35).

In contrast, a study published in 2018 evaluated the health impact of repetitive, chronic inhalation of e-cigarette vapor from devices other than JUUL (36). In the study, mice were exposed to e-cigarette vapor (E liquid containing PG/VG and nicotine with no flavor) daily for either three or six months. The findings showed that chronic e-cigarette vapor inhalation increased the levels of circulating inflammatory cytokines, altered cardiovascular function, as well as inducing cardiac, hepatic, and renal fibrosis (36).

Furthermore, in a comparative study, two identical devices were employed with the same e-liquid (PG/VG ratio, nicotine concentration, and flavors) but mounted with two different coils (1.5 and 0.25 ohm) to obtain total wattages of 8 ± 2W and 40 ± 5W, respectively (37). Interestingly, the study found that aerosols generated at higher wattages caused substantially more robust inflammatory responses in rats than aerosols generated at lower wattages (37). All of which indicate that the chemical profile created by each e-cigarette device and e-liquid, as well as the temperature and wattage applied to the e-liquid throughout the vaping and aerosolization process, all play important roles in modifying metabolic and immunologic profiles.

2. Cardiovascular Diseases-overview

2.1. Stroke & myocardial infarction

Cardiovascular diseases (CVD) remain a global disease burden with increasing incidence of prevalence, mortality and are a major contributor to disability over the last ten years of which, ischemic heart disease (IHD), clinically known as myocardial infarction (MI) and ischemic cardiomyopathy, and stroke are the most prevalent. More importantly, the number of CVD cases from 1990 to 2019 have doubled from 271 million to 523 million cases (38). MI occurs when blood flow to a region of the heart is disrupted, and the heart muscle is harmed due to a lack of

oxygen delivery and/or one of the coronary arteries that delivers blood to the heart becomes blocked as a result of an unstable buildup of plaques, white blood cells (WBCs), cholesterol, and fat (39). An underlying cause of acute myocardial infarct (AMI), as well as stroke, is atherosclerosis, which is a thickening of the arteries due to lipid deposition that can result in arterial narrowing as well as blood flow disturbance (26).

2.2. Atherosclerosis

2.2.1. Pathogenesis of atherosclerosis

Atherosclerosis is a multifactorial disease involving the interplay of genetic and environmental factors. Hyperlipidemic states, diabetes mellitus, smoking and hypertension are some of the risk factors for atherosclerosis (40). Dyslipidemia plays a central role in the development of atherosclerosis, which is characterized by increased low-density lipoprotein (LDL) levels and decreased high density lipoprotein (HDL) levels (40). HDL is known to be a key element in atherosclerosis because of its role in reverse cholesterol transport (40). In general, atherosclerosis is characterized by an accumulation of cholesterol, infiltration of macrophages, proliferation of smooth muscle cells (SMC), accumulation of extracellular matrix components and formation of thrombus (41)(Figure 1). The progression of atherosclerosis begins when the endothelial cells (EC) of the arterial wall become damaged, which can be caused by several factors including hypercholesterolemia. EC damage increases the permeability of the arterial wall allowing the LDL to enter the tunica intima. Normally, WBCs, such as monocytes, move freely through the blood vessels and do not attach to EC as the blood flows across them. However, when ECs are exposed to irritating stimuli, such as oxidised lipid, they become activated and express selectins and cell adhesion molecules (26). Selectins bind to their predominant ligand expressed on monocytes. This binding allows circulating monocytes to be

tethered and roll along the endothelium. Firm adhesion between monocytes and ECs is accomplished by the subsequent ligation of monocyte integrins with cell adhesion molecules on the ECs (26). This will be expanded upon in greater detail in section 2.2.2. Monocytes then migrate into the subendothelial space, where they differentiate into macrophages. Macrophages become activated and scavenge the oxidised lipoprotein particles and turn into foam cells that eventually accumulate and form the plaque. Vascular smooth muscle cells (VSMCs)then proliferate and eventually form a fibrous cap over the plaque, which results in a stable plaque

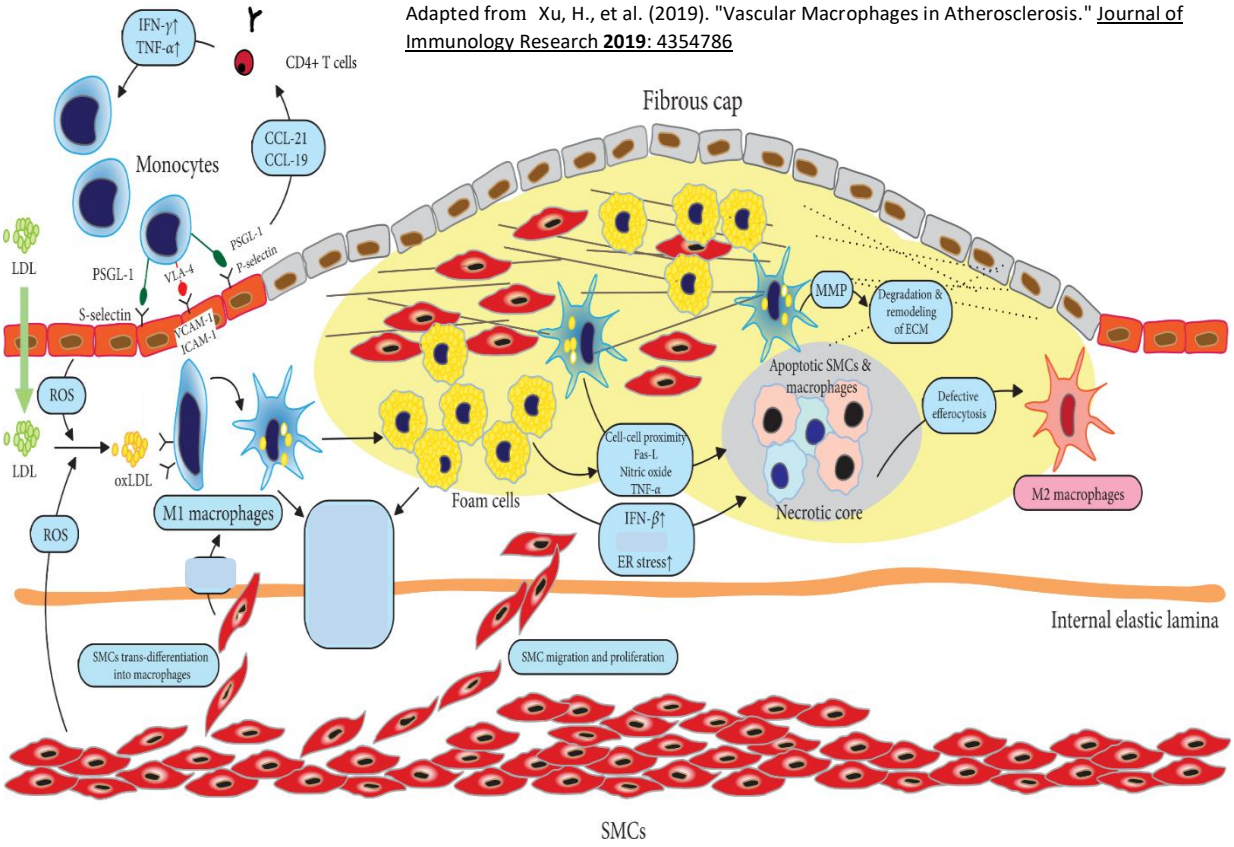

Adapted from Xu, H., et al. (2019). "Vascular Macrophages in Atherosclerosis." Journal of Immunology Research **2019**: 4354786

Macrophage infiltration is the initial step toward the development of an atherosclerotic plaque (42); their conversion into foam cells is responsible for the distinctive fatty streak seen in the early stages of atherosclerosis (43). The migration of SMC from the medial layer of the blood vessel wall into the intima marks the change from fatty streak to a more complicated lesion (44). Matrix metalloproteinase family (MMPs), particularly MMP-9, which is primarily generated by activated macrophages and VSMCs, are negatively linked to the stability of atherosclerotic plaques (45). As the atherosclerotic plaque grows, MMPs and other matrix-degrading proteases released mostly by inflammatory cells thin the fibrotic cap, increasing its fragility (46). Furthermore, when plaques develop necrotic cores (gruel plaques), the lesion's free cholesterol concentration rises while cholesterol esters fall; an increase in free cholesterol linked to lesion instability (47). Eventually, when the damaged plaque can no longer withstand the hemodynamic load, it ruptures, exposing its debris into the artery lumen and causing thrombus development (46).

Figure 1. The Pathogenesis of Atherosclerosis. Atherosclerosis is caused by lipid buildup in the subendothelial space. By attaching to active endothelial cells (ECs) and accessing the subendothelial cell space, circulating monocytes are attracted to the lesion site. Macrophages within the plaque absorb lipid deposit particles and convert into foam cells, resulting in the formation of early atherosclerotic lesions. Lesional macrophages cause a cascade of inflammatory reactions, including increased lipoprotein retention, extracellular matrix (ECM) modification, and long-term chronic inflammation. Oxidized LDL (oxLDL) also causes foam cell necrosis, which leads to the formation of a necrotic core and the instability and rupture of advanced plaques. Abbreviations: ER: endoplasmic reticulum; ICAM: intercellular adhesion molecule; IFN: interferon; IL: interleukin; MMP: matrix metalloproteinase; oxLDL: oxidized

2.2.2. Markers in the Development of Atherosclerosis Inflammation

There are various biomarkers that reflect early pro-atherogenic processes, including endothelial damage and activation mediated by adhesion molecules, which may be observed at

both cellular and circulation levels, and immune cell infiltration. When EC are activated, they produce monocyte chemoattractant protein-1, interleukin (IL)-8, intracellular cell adhesion molecule-1(ICAM-1), vascular cell adhesion molecule-1 (VCAM-1), E-selectin, P-selectin, and other inflammatory factors that attract lymphocytes and monocytes that bind to the endothelium and infiltrate the arterial wall, causing inflammation (48).This process involves several cells and cytokines, including macrophages, lymphocytes (T and B cells), dendritic cells (DCs), EC, VSMCs, IL , adhesion molecules, and tumour necrosis factor (TNF-α) (49). Among all these proinflammatory messengers that are released by immune and vascular ECs, herein, we are only addressing the few that have been investigated in our project.

A. Adhesion molecules

Adhesion molecules are proteins that have a role in cell identification, activation, and proliferation, as well as mediating tissue inflammation and immunological responses and participating in and regulating thrombosis (50). The adhesion molecules linked to atherosclerosis are in the immunoglobulin superfamily (IgSF), selectin family, and integrin family.

The IgSF has a chemical structure that is similar to immunoglobulins, and they operate as a receptor and ligand for the integrin family of adhesion molecules, which are important in cell identification and adhesion (50). Moreover, ICAM-1, VCAM-1, and platelet endothelial cell adhesion molecule-1 (PECAM-1) are the three primary types of IgSF. High levels of VCAM-1 and ICAM-1 enhance macrophage proliferation, resulting in a high number of macrophages aggregating in the plaque, thus enhancing plaque instability (51). PECAM-1 has the ability to oligomerise, which influences cellular activation and integrin activities. As a result, PECAM-1

plays a role in endothelial integrity and cell extravasation from the blood compartment into the artery and underlying tissue (52).

Selectins are transmembrane glycoproteins that primarily contribute to leukocyte rolling and adherence. Endothelium-selectin (E-selectin), platelet-selectin (P-selectin), and leukocyte selectin (L-selectin) are the three selectin types. P-selectin glycoproteinligand-1 (PSGL-1) is the main ligand of selectin. It is a dimeric polymer rich in O- and N-glycans that is expressed on nearly all leukocytes (53). The three selectins are named for their dominant site of expression: L-selectin is present in leukocytes, E-selectin in endothelial cells, and P-selectin on platelets but also in endothelial cells (54). Lymphocyte rolling is mediated by L-selectin, whereas P-selectin and E-selectin are largely produced during endothelial inflammation and assist monocyte, neutrophil, and lymphocyte rolling (55). Selectin activation, notably P-Selectin and E-Selectin, has been shown to have a role in both the early and late phases of atherosclerotic lesion formation (56). P-selectin expression is strongly linked with the degree of atherosclerotic lesions and plaques in clinical investigations (57, 58).

The integrin family is a glycoprotein receptor present on numerous cell surfaces, and as transmembrane receptors, integrins can connect the internal actomyosin cytoskeleton to IgSF counter-receptors (VCAM-1 and ICAM-1) on neighbouring cells (59). Very late antigen-4 (VLA-4) integrin -expressed on circulating monocytes- is a ligand of the VCAM-1 that is expressed on the surface of the EC and is activated by cytokines, while lymphocyte function-associated antigen-1 **(**LFA-1) is a ligand of the ICAM-1 (26). Integrin signalling may influence numerous facets of atherosclerosis, from the onset of inflammation to the formation of advanced fibrotic plaques (50).

B. Soluble adhesion molecules

Many cellular adhesion molecules have soluble forms in the circulation, such as sICAM-1, sPECAM-1, sP-selectin, and sE-selectin. Even though their pathogenic significance is unknown, levels of soluble adhesion molecules have been proposed to be helpful risk predictors of cardiovascular events in healthy populations and diverse disease contexts (60). Increased soluble form synthesis might be due to increased gene transcription, changes in mRNA stability, changes in translation, generation of alternatively spliced forms, or increased proteolytic cleavage from the cell surface (54). However, there is yet limited evidence on the link between the degree of cellular expression and the number of soluble forms (54).

Soluble adhesion molecule levels have been linked to a variety of cardiovascular risk factors, including smoking (61), hypertension (62), low HDL cholesterol (63), and hypercholesterolemia and/or hypertriglyceridemia (64, 65). Soluble adhesion molecules have been proposed as biohumoral indicators of the extent and severity of atherosclerosis. sICAM-1 has a strong relationship with carotid intima-media thickness, an indicator of early atherosclerosis (66). sICAM-1 was predictive of stroke risk in the Bezafibrate Infarction Prevention (BIP) trial of individuals with CAD (67). Furthermore, in a prospective epidemiological study of apparently healthy women, high baseline levels of soluble P-selectin were related with increased risks of future myocardial infarction, stroke, coronary revascularization, and cardiovascular mortality (68). In the same study, cigarette smoking was directly related to higher levels of soluble P-selectin (68). Furthermore, elevated sE-selectin levels predict restenosis following percutaneous transluminal angiography (69).

C. Inflammatory components

Over the last several decades, research has revealed that an atherosclerotic lesion is distinguished not only by cell proliferation and cholesterol accumulation, but also by immune cell infiltration, mostly of monocyte-derived macrophages, T cells, and myeloid lineage cells such as DCs and neutrophils. Macrophages, the main immune cell population in arterial plaques, have been found to be associated in the immunological responses and development of atherosclerosis (70, 71). Macrophages are mainly generated from circulating monocytes generated from the bone marrow (72) or spleen (73) in response to tissue damage, infections, or proinflammatory cytokines and chemokines (26). Macrophages are categorised into immune-activated proinflammatory macrophages (M1) and immunomodulatory alternatively-activated macrophages (M2). M1 macrophages are commonly polarised by Th1 cytokines, such as interferon (IFN-γ) and TNF, as well as pathogen-associated molecular complexes (PAMPs), such as lipopolysaccharides and lipoproteins (74), while M2 macrophages are mostly activated in response to Th2-related cytokines, such as IL-4, IL-33, and IL-13 (75). M1 macrophages generate proinflammatory cytokines, such IL-6, IL-12, IL-23, TNF-α and IL-1β, and low levels of IL-10 (76, 77). Persistent M1 macrophage activation can activate the NADPH oxidase system and create ROS and nitric oxide, causing chronic tissue damage and impeding wound healing (78). M2 macrophages are required at this stage to counteract the proinflammatory response and control inflammation, scavenge apoptotic cells, accelerate angiogenesis and fibrosis, and promote tissue repair (75). Furthermore, recent research has discovered that M1/M2 macrophage ratio influences atherogenicity. Cells in mouse atherosclerotic plaques show M1 and/or M2 markers, and it has been proposed that plaque progression is associated with phenotypic shift from M2 to M1 (79, 80). On the other hand, studies in hypercholesterolemic mice showed that decreased atherosclerosis was associated with shifting from M1 to M2 (81, 82), whereas knocking down

the IL4 gene, that is known to promote M2 polarisation, causes plaque regression (83). Together, this suggests that the ratio of M1 and M2 macrophages is critical for plaque progression/regression.

DCs are antigen-presenting cells (APCs) that play a role in the genesis and progression of atherosclerosis. They are seen in healthy aorta but increase in number as the illness progresses (84, 85). $CD11b^+$ DCs are the most prevalent DC subgroup observed in the mouse aorta, especially in the intima (86). $CD11b^+$ DCs are distinguished by the production of cytokines, such as IL-6 (87) and IL-23 (88). Furthermore, during atherogenesis, $CD11b^+$ DCs have been observed to quickly proliferate in mice atherosclerotic plaques (89).

Neutrophils, the most common and essential cells in innate immune responses, have long been thought to be indicators of cardiovascular disease. Circulating neutrophil levels in humans are predictive of future unfavourable cardiovascular events (90, 91). In mice, the quantity of circulating neutrophils corresponds with the size of growing lesions (92). In atherosclerotic settings, neutrophils were found to accelerate all phases of atherosclerosis by promoting monocyte recruitment, macrophage activation, and cytotoxicity (93).

T cells consist mainly of $CD4^+$ and $CD8^+$ cells. $CD8^+$ T cells and $CD4^+$ T cells induce immunological responses to peptides presented by Major Histocompatibility Complex (MHC) Class I on all nucleated cells and MHC Class II on APCs, respectively. T cell activation and clonal proliferation are caused mainly by the simultaneous binding of a particular T cell receptor (TCR) with co-stimulatory signals produced by APCs (94). Besides its adhesion functions (discussed in section 2.2.2A), PSGL-1 interacts with chemokine ligand (CCL) 21 or CCL19 and efficiently attracts activated $CD4^+$ and $CD8^+$ T cells, that produce IFN-γ and TNF-α contributing in the proinflammatory environment (95, 96).

CD4+ T cells are classified into subpopulations of helper T (Th), and for the purpose of this thesis, we will focus on Th1, Th2, and regulatory T cells (Tregs) only. Several investigations have indicated that Th1 cells aggravate atherosclerosis and are the most prevalent Th cell subgroup in plaque (97, 98). Th1 cells secrete IFNγ and express T-box transcription factor TBX21 (T-bet) and chemokine receptors (CCR), such as CXC- CXCR3 and CC- CCR5 (99). Furthermore, many $CD4^+$ T cells in the atherosclerotic plaque also express other Th1-associated pro-inflammatory cytokines, such as IL-2, IL-3, TNF-α, and lymphotoxin, all of which can activate macrophages, T cells, and other plaque cells and thus, accelerate the inflammatory response (100). IFNγ may diminish plaque stability directly by decreasing VSMC proliferation (101), affecting macrophage polarization (102), and regulating cardiovascular risk factors (103).

Th2 cells produce atheroprotective cytokines including IL-4, IL-5, and IL-13(99). In apolipoprotein E (Apoe) knockout mice ($Apoe^{-/-}$), IL-4 inhibits Th1 cell responses and reduces atherosclerotic lesion formation (104). Furthermore, in $LDLr^{-/-}$ mice fed a high-fat diet, IL-13 administration was found to modulate established atherosclerotic lesions by increasing lesional collagen content and decreasing VCAM-1 expression, leading to decreased macrophage infiltration in plaques compared to the control group (105). In humans, plasma IL-5 levels were found to be inversely related to carotid intima media thickness (106, 107).

The suppressive function of Tregs is achieved through the expression of the forkhead/winged helix transcription factor FOXP3 (108, 109). Tregs have the distinct impact of impairing T cell proliferation and cytokine generation from other T cell subsets, despite activation of their antigen-specific T-cell receptors. Tregs carry on their inhibition function through a variety of ways, including the production of suppressive cytokines, such as IL-10, TGF-α, or IL-35 (110). Tregs are powerful atheroprotective cells; they play essential roles in the suppression of

inflammation and the control of adaptive immune responses (111). Tregs have been found in normal aortic tissues of mice and humans, and their levels are lower in atherosclerotic animals and cardiovascular patients when compared to healthy controls (112, 113).

$CD8^+$ T cells, the other major subset of T cells, differentiate into cytotoxic T cells when they recognize their antigens (114). CD8 cytotoxic activity is associated with cytokine release, mainly IFN-γ and TNF-α, to induce apoptosis and inflammation. In addition, $CD8^+$ T cells secrete cytotoxic granules, in particular perforin and granzymes, inducing lysis of target cells (114). CD8+ cells, but not CD4+ cells, were activated and produced cytokine in the spleen of $Apoe^{-/-}$ mice on a high-fat diet for a month. This suggests that $CD8^+$ T cell activation predominates early immune responses to hypercholesterolemia (115). $CD8^+$ T cells promote atherosclerotic lesion development in a variety of ways, including mobilising granulocyte and monocyte progenitors in the bone marrow and spleen through IFN-γ. This action results in increases in circulating Ly6C monocytes, which then moves into vascular tissues and develops into proatherogenic macrophages (116). Together, atherosclerosis progression and regression are highly associated with pro-inflammatory and anti-inflammatory markers, respectively.

2.2.3. Atherosclerotic mouse models

The pathogenesis of atherosclerosis in humans is a complicated process driven by a variety of risk factors such as ageing, hyperlipidemia, hypertension, and diabetes, which results in immunometabolic dysregulation (40). Thus, the investigation of the immunometabolic processes and molecular mechanisms underlying atherosclerosis demands the use of animal models that replicate human pathophysiology. However, due to their drastically different lipid profile from humans, mice are highly resistant to the development of atherosclerosis (117, 118).

As a result, genetic modification of their lipid metabolism is required. Over the last few decades, several animal models for atherosclerosis research have been investigated. Although each model has strengths and weaknesses, depending on the focus of the research, different animal models can be chosen.

Atherosclerosis-prone mouse models were created by targeting various genes. All these mouse models cause atherosclerosis by changing the lipoprotein profile toward increasing VLDL- and LDL-cholesterol content, resulting in a lipoprotein profile equivalent to humans (119-123). The most well-known atherosclerotic mouse models are Apoe$^{-/-}$ mice, low density lipoprotein (LDL) receptor deficient mice (LDLr$^{-/-}$), and the (PCSK9) mouse model (124). Each of these models are further described below.

(Apoe$^{-/-}$) mice model: Apoe is a glycoprotein synthesized mainly in the liver, which acts as a structural component of all lipoprotein particles except low-density lipoproteins. Moreover, it is involved in cholesterol homeostasis, local redistribution of cholesterol within tissues, immunoregulation as well as dietary absorption and biliary excretion of cholesterol (125, 126). In Apoe$^{-/-}$ mice, the deletion of the Apoe gene was carried out in mouse embryonic stem cells by homologous recombination (127). This process is utilised just once for producing these mice, after which, users can breed the mice to produce more generations. Deletion of the Apoe gene impairs the ability of mice to clear plasma lipoproteins resulting in plasma cholesterol levels of 400–800 mg/dl even when mice are on normal rodent chow diets. In addition, plasma cholesterol is increased fourfold in Apoe$^{-/-}$mice fed Western-type diets (128). As a result, Apoe-deficient mice develop hyper- and dyslipoproteinemia, severe hypercholesterolemia, and atherosclerotic lesions as soon as a few weeks after birth (129). Another advantage in Apoe$^{-/-}$mice is the presence of the whole series of atherosclerotic lesions (127). After 6 weeks of

age, the attachment of monocyte to endothelial cells was observed, while after 8 weeks the development of foam cell lesion was noticed. In addition, the presence of intermediate lesions was detected after 15-20 weeks, largely containing SMC and fibrous plaques that were composed of SMCs, extracellular matrix and a necrotic core covered with a fibrous cap (128).

Although this mouse model is used by many research groups, it has some drawbacks. Apoe is synthesized not only in the liver, but also in the brain, where it is involved in neural health and damage recovery (130). *In vitro,* Apoe has been shown to impact neuronal survival (131), morphology (132, 133), and adhesion (133), as well as increase smooth muscle cell proliferation and supress microglia inflammatory responses (134, 135). In vivo, a study published in 2001 sought to investigate the functions of Apoe within the nervous system by examining $Apoe^{-/-}$ mice (130). In the study, they observed functionally compromised blood–nerve and blood–brain barriers (BNB,BBB) in $Apoe^{-/-}$mice, highlighting the significance of Apoe in BNB/BBB integrity (130). It has recently been demonstrated that the impact of Apoe on BBB integrity and cerebral blood flow is isoform-dependent (136-138). Apoe4, one of the Apoe isoforms, has been linked to increased risk and decreased age of onset of familial and late-onset Alzheimer disease (AD) (139). This interplay of Apoe activities in the liver and brain makes distinguishing the distinctions in CVD and other systems challenging.

Moreover, in $Apoe^{-/-}$ mice, the most abundant lipoprotein is VLDL, unlike in humans where LDL is the most abundant (140). Finally, it was found that the incidence of plaque rupture and thrombosis is negligible in $Apoe^{-/-}$ mice (140). These events are one of the common underlying causes of MI and stroke in humans (127), thus this is a barrier in understanding the concepts of plaque rupture and its complications in humans.

LDL receptor-deficient (LDLr$^{-/-}$) mice model: The LDL receptor is a membrane receptor that mediates the endocytosis of cholesterol-rich LDL, hence maintaining LDL levels in the plasma (129). To produce mice that lack a functional LDL receptor, homologous recombination technique was used in cultured embryonic stem cells (120). LDLr$^{-/-}$ mice have human-like lipid profiles as plasma cholesterol is mostly carried by LDL particles in this model (129). Another strength of LDLr$^{-/-}$ mice is that the omission of the LDL receptor has no effect on inflammation when compared to Apoe deficiency. As a result, the development of atherosclerotic plaque is based primarily on increased lipid levels in plasma with no regard to any other functions related to LDLr (117, 141).

Although this mouse model is widely used in research, it has some disadvantages. When fed a chow diet, LDLr$^{-/-}$ mice have only slightly higher plasma cholesterol levels than wild-type mice and develop no or very moderate atherosclerosis (129). To overcome such limitations, mice must be fed high-fat/high cholesterol Western-type diets as they are found to significantly increase lipoprotein levels with great incidence for atherosclerotic lesion development (129). Moreover, as in the case with Apoe$^{-/-}$ mice, this model lacks spontaneous plaque rupture, thrombosis, and complications (129).

PCSK9-AAV mice model: PCSK9 is a serine protease that is highly expressed in the liver and intestine with lower levels of expression observed in the kidney, spleen, and aorta (142). It functions by regulating lipid metabolism by binding to the epidermal growth factor-like-A domain of the LDLr on the hepatocyte surface, where it is endocytosed along with the receptor, interfering with its ability to recycle to the plasma membrane. Instead, the receptor is directed to the lysosome where it is degraded, leading to decreased levels of the receptor thus decreased internalization of LDL (142). Dysregulation of this pathway by gain-of-function mutations in

PCSK9, such as amino acid substitution of Asp374 by Tyr (D374Y or DY), that increases the affinity of PCSK9 for the LDLr by ≥10-fold (143), is linked to hypercholesterolemia and atherosclerosis in humans and mice (144-146). Expression of recombinant AAV vectors containing the human $PCSK9^{DY}$ variant results in long-term transgene expression in many animal models (147-149). Therefore, a single injection of recombinant adeno-associated virus (rAAV) encoding gain-of-function mutant forms of PCSK9 is sufficient to cause downregulation of LDLr inducing hyperlipidemia and atherosclerosis in mice, in which plaque formation is similar to what is found in humans (123, 150). One major advantage of AAV-mediated transexpression is its robust stability after a single administration. Furthermore, the clear association between hyperlipidemia and atherosclerotic lesion development in the AAV-$PCSK9^{DY}$ model could be easily used to test different scientific questions without the need for tedious, costly, and time-consuming backcrosses (123). Another advantage of the AAV-PCSK9 model that we are particularly interested in is that we can control the time of atherosclerosis induction to evaluate the impact of JUUL in various scenarios that mimic human outcomes.

Despite the appealing advantages of this model, it does have some limitations. PCSK9 model is slower than other models to develop atherosclerotic plaques. Two months following a single intravenous injection and on a chow diet, $PCSK9^{DY}$-AAV mice plasma cholesterol levels were found to barely reach 316 mg/dl (123), whereas $Apoe^{-/-}$ mice (age 6-10 weeks) on a chow diet had plasma cholesterol levels averaging 600 mg/dl (128). However, in PCSK9 mice fed Western-type diets for 2 weeks, their hyperlipidemia was found to be exacerbated with plasma cholesterol levels up to 1165 mg/dl (123); indicating that high fat diets could be used to overcome such limitation. Another limitation is that this model is incapable of simulating

genuine late-stage atherosclerosis events in terms of plaque rupture, thrombosis, and consequences (129), a limitation shared with Apoe$^{-/-}$ and LDLr$^{-/-}$ mice models (127, 129).

3. Electronic Cigarette and Atherosclerosis

Tobacco use is responsible for more than one out of every ten fatalities from cardiovascular disease each year (151). Given the close link between tobacco cigarette smoking and cardiovascular illness, there is reason to be concerned about the cardiovascular risks of e-cigarettes. Increased oxidative stress and inflammation are key processes in the development of atherosclerosis and cardiovascular risk (152). Recent studies have found that acute and chronic exposure to e-cigarette aerosol induced lung and systemic inflammation, respectively (34, 36). Furthermore, many e-cigarette and JUUL pod flavours were shown to enhance cellular ROS and mitochondrial superoxide generation in bronchial epithelial cells and monocytes, resulting in elevated inflammatory mediators such IL-6, IL-8, and prostaglandin E2 (PGE2) (12, 153). Similarly, flavored JUUL exposure was found to alter the levels of oxidative markers in the circulation, 8-hydroxy-2'-deoxyguanosine (8-OHdG) and malondialdehyde (MDA), thus inducing systemic oxidative stress in flavoured-based manner (34).

A few studies have found that e- cigarettes correlate with MI (154, 155), yet no causation was defined. Moreover, little knowledge exists on the impact of JUUL vaping on the cardiovascular system. In addition, the effects of vaping in mouse models of atherosclerosis remain controversial. Interestingly, Apoe$^{-/-}$ mice exposed to vaping a nicotine-containing product and fed high fat diets for 12 weeks showed a striking increase in plaque size (156). Controversially, another study (funded by the tobacco conglomerate Philip Morris) showed no significant difference in plaque size after 3 and 6 months of vaping exposure (157).

In many studies using *in vitro* cell-based approaches and animal models, interpretation is confounded because of differing regimes of exposure and device/e-liquids used. Moreover, most studies fail to report on correlation with human puff topography (*i.e.,* puff volume, puff interval, *etc.*) and objective measurements of exposure (*e.g.,* cotinine) (7). In short, there is a paucity of studies using JUUL that have rigorously evaluated the health risk associated with product use. Therefore, we will use our preclinical exposure model to test whether inhalation of aerosolized JUUL e-liquids causes cardiovascular damage**.**

4. Rational and Hypothesis statement

Despite the increase in pod-style e-cigarette (i.e. JUUL) use among youth, the health effect of JUUL use among never-smokers continues to be largely unknown (2). In addition, e-cigarette vascular effects, in particular atherosclerosis, remain controversial (156, 157). JUUL product exposure has never been studied in a pre-clinical model of atherosclerosis. We recently reported that a short (3 day) inhalation exposure of flavoured JUUL e-cigarette aerosols alters the basal immune cell components and induces oxidative stress responses, both of which could be pro-atherogenic (34). At this early time (4 week), pro-atherogenic changes would be predicted to enhance CVD later in life and add to other risk factors contributing to atherosclerosis. Having established our exposure model of human vaping, we hypothesized that there will be early adverse pro-atherogenic outcomes following JUUL aerosol exposure including vascular and immune modifications in a hyperlipidemic mouse model.

Chapter Three: Methods and Materials

3.1 Animals.

C57BL/6J mice were purchased from the Jackson Laboratory and bred in-house. Male mice were used in these experiments since they have higher levels of plasma PCSK9 than females and require less amount of virus to be injected (10 mice per group were used, 4 weeks old) (142). The McGill University Animal Care Committee authorised all operations, which were carried out in compliance with the Canadian Council on Animal Care Committee.

3.2 JUUL products.

For this study, we used commercially available JUUL products containing 59 mg/mL nicotine. Mango-flavored pod cartridges were obtained from a local vape store. For all exposures, a regular commercial JUUL device was utilised. The vehicle control, which was made up of a 30:70 ratio of propylene glycol (PG) and vegetable glycerin (VG), was purchased from Fusion Flavours (fusionflavours.ca).

3.3 Animal exposures.

Mice were injected intraperitoneally with 3×10^{10} AAV-PCSK9 viral particles (GeneCopoeia, Inc., Cat# AA08-50004-01-1000) , which was generated from a MegaPrep of plasmid (Addgene, pAAV/D377Y-mPCSK9, Cat# 58376),(Omega, Plasmid DNA Maxi kit, Lot# D692218341-28) . On the same day as injection, mice were started on a high-fat diet (ENVIGO high fat diet, TD.10825). One week following the injection, mice were randomly allocated to one of three groups: air, vehicle (PG/VG) or JUUL (Mango). Air-exposed mice did not receive any other exposures in the system except for air. Exposures were performed using the SCIREQ® inExpose™ system equipped with an extension for JUUL (Figure 2). Exposure parameters and the

puff profile were programmed using the flexiWare software. Mice were exposed to a puff regime consisting of three 20-minute exposures per day for 4 weeks. The puff regime was 4 puffs per minute with a 78 mL puff volume, 2.4 second puff duration, and three hours between exposure sessions. These puff topography and usage parameters are consistent with human use patterns of e-cigarettes (18, 158, 159). To establish a baseline for the hyperlipidemic mice, wild-type C57BL/6J mice exposed to air only were used to serve as a negative control group for some findings. Following the 4 weeks of exposure, mice were euthanized with isoflurane, and the

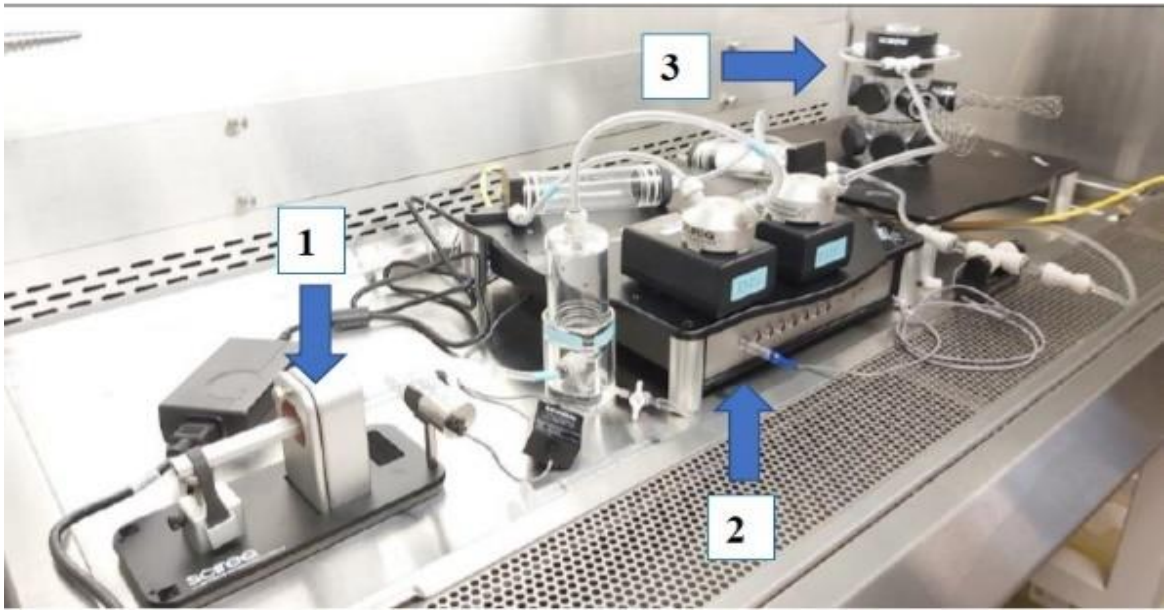

Figure 2. Inhalation exposure system. JUUL extension (1), pump unit (2) and nose-only tower for mice (3).

aorta, heart, spleen, liver, and kidneys were dissected and collected.

3.4 Assessment of atherosclerotic lesion.

The atherosclerotic lesions and lipid content were evaluated within the heart aortic sinus. The heart was removed, rinsed in PBS, fixed in 4% paraformaldehyde for 24 hours, then incubated overnight in a 30% sucrose solution. The tissues were then cut horizontally with the sinus facing

up when embedded in Tissue Tek OCT reagent, and serial cryosections of 7-µm thickness were cut from the origin of the aortic root throughout the aortic sinus. Seven to ten sections per animal were placed on 10 different slides. Thus, individual slides contained between 7 and 10 slices stained with oil red O (Electron Microscopy Sciences, 0.5%500ml, Cat#266090) for 40 minutes, rinsed with deionized water, then mounted with Immunomount (Thermo scientific #9990402). Images were obtained using INFINITY CAPTURE software and camera (Lumenera) and analysed by calculating the mean lesion area using ImageJ software (National Institute of Health). Percentage of lesion area was evaluated relative to the total aortic sinus area. Percentage of lipid content in sinus plaque was evaluated with ImageJ by evaluating the percentage of oil red O staining per plaque area.

3.5 Immunohistochemistry (IHC) staining.

VCAM-1 expression on the endothelial walls of the carotid and brachiocephalic artery (BCA) arteries was evaluated using IHC staining. Arteries were dissected and rinsed with PBS and fixed in 4% paraformaldehyde, embedded longitudinally in paraffin, and processed. Then, consecutive 4 μm ring sections of the arteries were sliced. Paraffin embedded arteries slices were deparaffinized with xylene 3 times for 5 minutes each and hydrated with an ethanol gradient (100%–70%). Slides were dipped 2 times in 100% EtOH for 5 minutes each, one time in 95% EtOH and one time in 70%EtOH for 5 minutes each, then washed under running tap water for 5 minutes and MQ H2O for 2 minutes. Antigen retrieval was performed using antigen retrieval solution (1X TRIS/EDTA pH 9 and Tween-20(100%)) in a pressure cooker for 20 min. After, slides were washed twice 5 minutes each with wash buffer (TBS plus 0.025% Triton X-100). Slides were then incubated in 4.5% H_2O_2 in 24 mM NaOH for 30 minutes and then rinsed 3 times with the wash buffer 5 minutes each. Then, slides were blocked in 10% goat serum

(Jackson Immuno Research, Lot no. 141655) with 1% BSA in TBS for 30 min and washed once. After, slides were incubated in Fc block plus mouse HRP (NA931V ECL antibodies, lot no. 17288406) (1:100) for 30 min followed by incubation with the primary antibody VCAM-1 (1:400) (Abcam, Cat#Ab134047) diluted in TBS with 1% BSA at room temperature for 30 min. After, slides were rinsed with wash buffer twice 5 minutes each and incubated with the corresponding secondary antibody (DAKO Envision+ HRP-ani rabbit) (DAKO, Cat# K4003) for one hour then washed 4 times with wash buffer 5 minutes each. Next, a short incubation of 1 minute with DAB substrate was used to visualize the VCAM-1 staining, followed by 20 sec of hematoxylin to counterstain. Finally, slides were dehydrated by being dipped once in 95% EtOH for 1 minute, twice in 100% EtOH 30 seconds each and 3 times in xylene 15 second each, then slides were mounted using Permount mounting media. Tissues were visualized using automated digital microscopy system (AxioScan slide scanner, Serial# 4631000289) and analyzed using (QuPath-0.2.3) by measuring the mean DAB Optical Density exclusively in the ECs.

3.6 Measurement of endothelial cell activation markers.

Blood (≈0.4 ml) was drawn by cardiac puncture and plasma samples were isolated using EDTA-coated tubes. E-selectin, P-selectin, ICAM-1, and Pecam-1 levels were assessed using an immunoassay kit (multiplex bead-based, mouse Cardiovascular Disease Panel 1 7-Plex Discovery Assay® Array (MDCVD1); EVE technology, Calgary, AB. Canada).

3.7 Measurement of total cholesterol and LDL levels.

Blood (≈0.4 ml) was drawn by cardiac puncture and plasma samples were isolated using EDTA-coated tubes. Total cholesterol, LDL, HDL, triglyceride, and glucose were assessed using Bio-Rad Liquid Assayed Multiqual kit (The Centre for Phenogenomics, Cat# 694 and 696, Toronto, Canada).

3.8 Measurement of cotinine levels.

Blood (≈0.4 ml) was drawn by cardiac puncture and plasma samples were isolated using EDTA-coated tubes. Serum cotinine levels were measured using an ELISA (Origene) as per the manufacturer's instructions.

3.9 CYP2A5 western blot.

CYP2A5 levels in the liver were investigated using western blot. Frozen liver samples were ground to powder using liquid nitrogen, then incubated for 30 minutes in RIPA lysis buffer (Bio Basic, cat# RB4478) containing protease (Roche, cat# 11873580001) and phosphatase inhibitors (Roche, cat#04906837001). After preclearing the lysates with centrifugation for 20 min at 13000 rpm, the amount of protein in each tissue lysate was quantified using a Bradford assay (Bio Rad, cat# 5000006). Then, an equal amount of protein (25 µg) from each sample was loaded and electrophoresed through a 7.5% SDS-PAGE polyacrylamide gel overnight. Proteins were then transferred to a PVDF membrane, which was previously activated by soaking it in methanol for 5 minutes, and blocked for 1 hour with 5% fat free milk in Tris-buffered saline with Tween-20 (TBST). Membranes were then incubated with human CYP2A6 primary antibody, which cross-reacts with murine CYP2A5 (1:500) (Proteintech, Cat# 21721-1-AP) at 4°C overnight, and rabbit anti-GAPDH (1:3000; used as a control loading protein, Cell Signaling Technologies, cat# 2118S). Membranes were then washed three times with TBST for 10 minutes each. Membranes were then incubated with secondary antibody (HRP-conjugated anti-rabbit, Cytiva cat#NA934V) (1:3000) for 2 hours at room temperature followed by washing three times with TBST for 10 minutes each. Signals were detected using prime ECL plus (Cytiva, cat# RPN2106) and the

membrane was exposed to an X-ray film (Thermo Scientific). Quantification and analysis of the expression of CYP2A5 and GAPDH were performed using ImageJ software.

3.10 Isolation of immune cells.

The spleen was dissected and placed in a 1.5 ml Eppendorf filled with cold PBS. A single cell suspension was obtained by gentle pressure-dissociation of spleen in PBS using a pestle, and then passed through a 70-µm sterile cell strainer. Spleen cells were centrifuged 10 min at 300 × *g*, 4°C after the filtration step. The pellet was resuspended in 1ml freezing media (10% DMSO, 90% FBS), then were cryopreserved at -80^{o}C.

3.11 Immunophenotyping by Flow cytometry.

Two panels were used to study both the myeloid and lymphoid lineages of hematopoietic immune cells: Myeloid and T-cell panels. Anti-mouse antibodies used for flow cytometric analyses are described in Table 1. Unstained cells were used as a negative control in all experiments. Unstained controls and fluorophore-minus-one (FMO) controls were utilized to establish baseline gate settings for each respective antibody-fluorophore. The correct dilutions of the antibodies to give efficient staining were established by titration of the antibodies.

Myeloid Panel			
Antigen	**Clone**	**Fluorochrome**	**Supplier, cat. no.**
CD45	30-F11	BUV395	BD Biosciences, 564279
CD11b	M1/70	e450	eBioscience, 48-0112-82
MHCII	M5/114.15.2	BV650	BD Biosciences, 563415
CD11c	HL3	BV786	BD Biosciences, 563735
Ly6G	1A8	FITC	BD Biosciences, 561105
F4/80	BM8	PE	eBioscience, 12-4801-80
Ly6C	AL-21	PE-CF594	BD Biosciences, 562728
CD19	MB19-1	APC	eBiosciences, 17-0191-81

Extended T-Cell Panel			
Antigen	**Clone**	**Fluorochrome**	**Supplier, cat. no.**
CD25	PC61	BV786	BD Biosciences, 564023
CD4	RM4-5	PerCP-e710	eBioscience, 46-0042-80
CD3	145-2C11	FITC	BD Biosciences, 553062
CD8	53-6.7	APC-e780	eBioscience, 47-0081-82
FoxP3	FJK-16s	APC	eBioscience, 17-5773-82

Table 1: Flow Panels Antibodies

3.11.1 Extracellular and intracellular staining.

Cells were defrosted and rinsed in cold PBS, centrifuged at 1500 rpm for 5 minutes at 4°C, and decanted. Cells were counted using trypan blue and then seeded at 1x 10^6 live cells per well using 96-well V-bottom plate. Each sample was then incubated with 50 µl Live/Dead stain (Thermo Fisher Scientific, L34966) for 30 minutes in dark at 4 °C. An amount of 100 µl PBS buffer was then added to each sample. Samples were centrifuged for 5 minutes at 1500 rpm and decanted. Samples were then blocked in 25 µl Fc blocking solution for 30 minutes in the dark at 4 °C; Fc block was used to block binding of antibodies to Fc receptors. Next, 25 µl of the respective extracellular antibodies of full stain or FMO's were added to the blocking solution (Table 1) and 25 µl FACS buffer was added to the well with the unstained sample. Samples were then incubated for 30 minutes in the dark at 4 °C. PBS (100 µl) buffer was then added to each sample. Samples were centrifuged for 5 minutes at 1500 rpm and decanted. After the samples were washed with FACS buffer, 100 µl Cyto Fix/Perm solution was added (Invitrogen, cat# 00-

5523-00). Samples were centrifuged for five minutes at 1500 rpm and decanted. of PBS buffer (100 µl) was then added to each sample. Samples were centrifuged for 5 minutes at 1500 rpm and decanted. Permwash solution (100 µl) was then added to each sample (Invitrogen, cat# 00-8333-56). Samples were centrifuged for 5 minutes at 1500 rpm and decanted. Next, 50 µl of the respective intracellular antibodies diluted in permwash solution was added and incubated for 30 minutes in the dark. Permwash solution (100 µl) was then added to each sample. Samples were centrifuged for 5 minutes at 1500 rpm and decanted. Samples were then washed with 100 µl FACS buffer, centrifuged for 5 minutes at 1500 rpm and decanted. Finally, pellets were resuspended in 150 µl FACS buffer and were then acquired using the BD LSRFortessa (BD Biosciences, Lady Davis Institute Flow Cytometry Core). Flow cytometry data were then analyzed using Flowjo 10.7.

3.11.2 Immune cell markers and Gating strategy.

For both Myeloid and T cell panels, forward scatter-H vs forward scatter-A were used to gate out single cells only. In the initial staining we tried cryopreservation then stain with Live/Dead to discriminate dead cells. However, we found that slightly overestimated the number of dead cells due to cryopreservation. So, in later runs we stained with Live/Dead prior cryopreservation and results were equivalent between runs. The expanded gating strategy schemes for immune-cell types are shown in Figures 3 and 4, and Table 2.

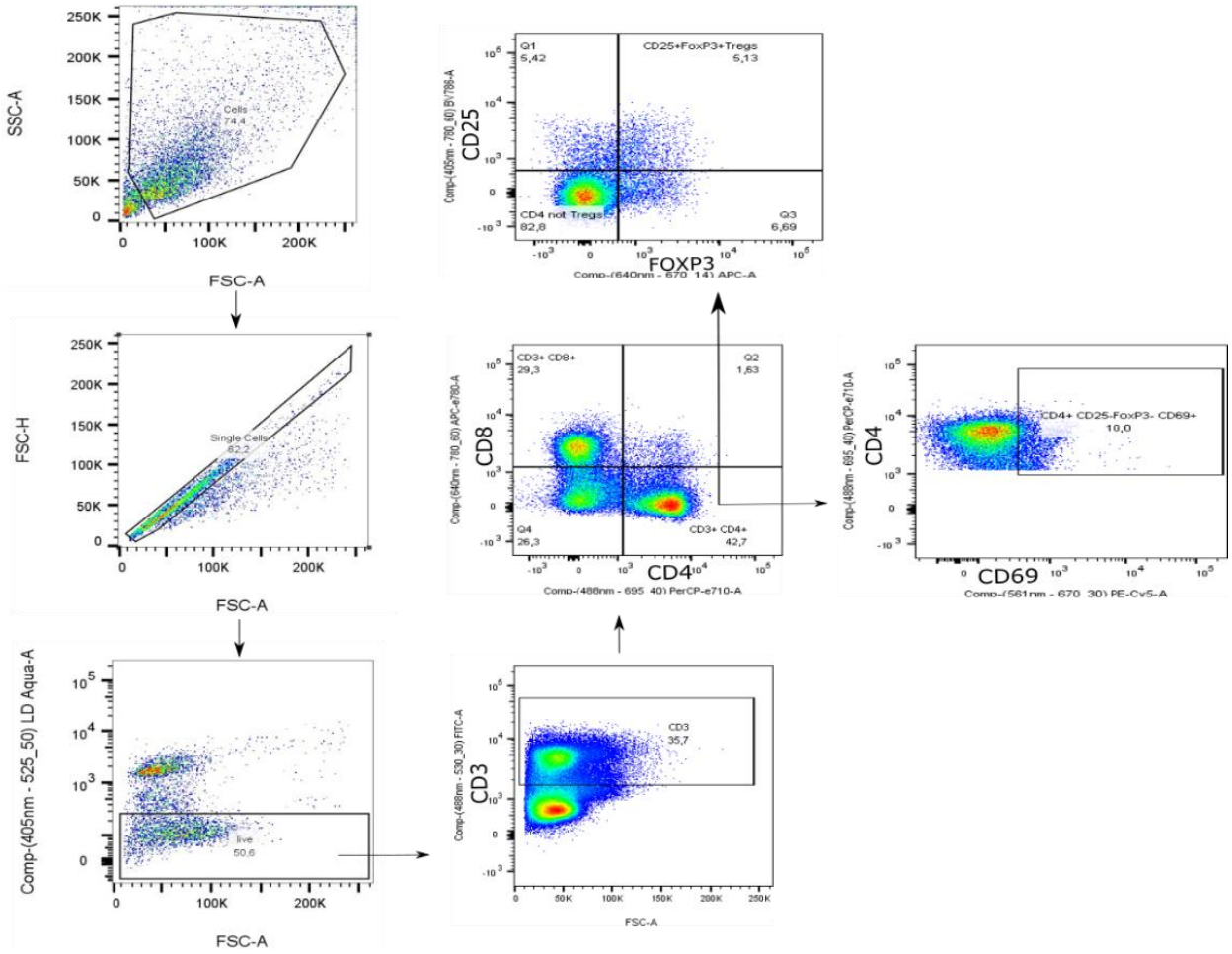

Figure 3. T-cell panel gating scheme. By performing immunophenotyping, T- cell panel was used to evaluate lymphoid lineages of hematopoietic immune cells

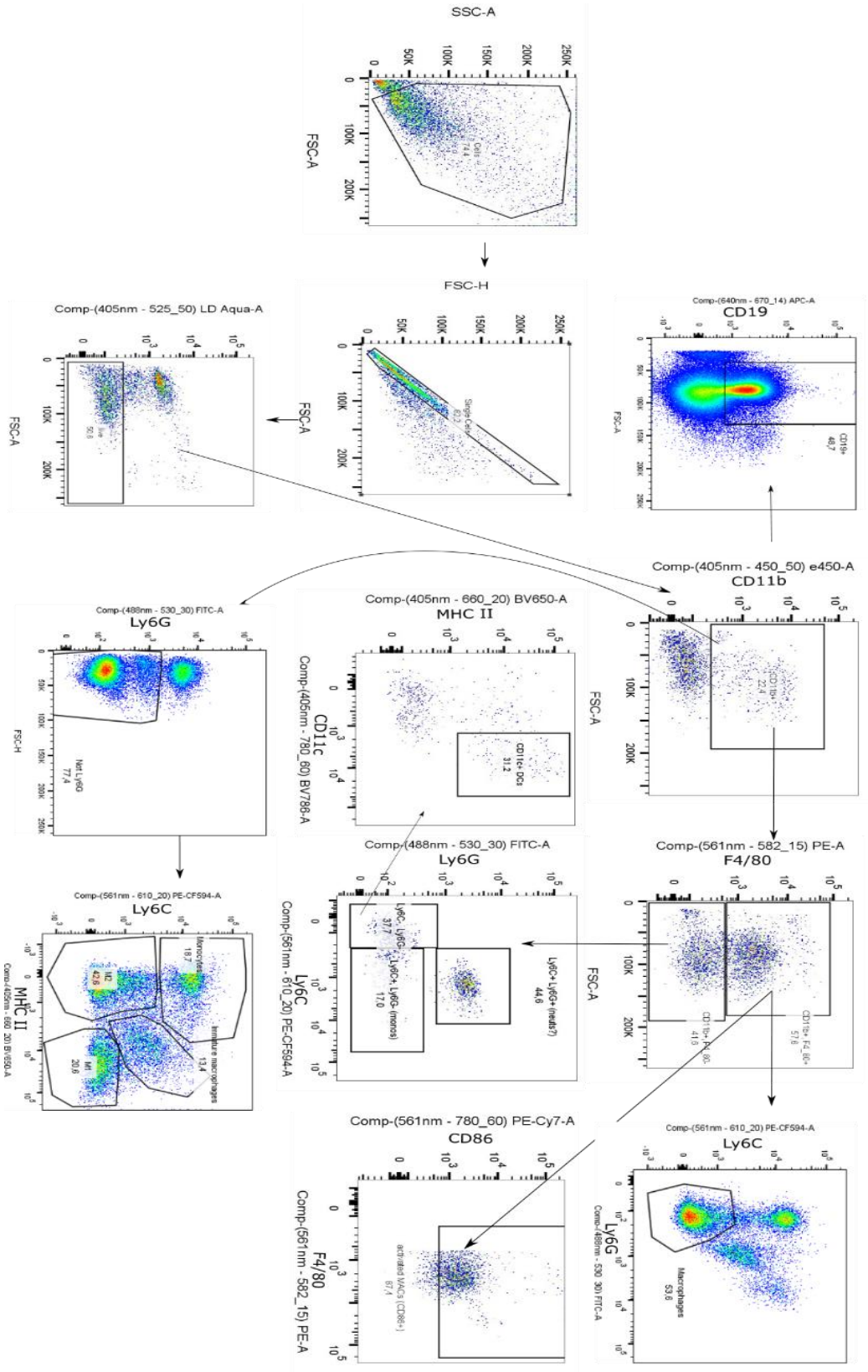

Figure 4.Myeloid panel gating scheme. By performing immunophenotyping, myeloid panel was used to evaluate myeloid lineages of hematopoietic immune cells

Myeloid panel	
Marker	**Used To**
CD11b	Define the myeloid lineage cells
MHC II	Separate different populations of macrophages and dendritic cells
CD11c	Marker for dendritic cells
Ly6C	Separate out monocytes and early-stage macrophages from mature macrophages
F4/80	Marker for macrophages
Ly6G	Marker for neutrophils
CD86	Marker for activated macrophage populations
CD19	Marker for B cells
T cell panel	
CD4	Marker for T helper cells
CD8	Marker for cytotoxic T
CD3	Isolate T-cells from the lymphocyte
CD4, CD25, and FOXP3	Identify regulatory T cells

Table 2: Flow Panels gating strategy

3.12 Statistical analyses.

Statistics were performed using GraphPad Prism, version 8.00 (GraphPad Software, San Diego CA). The Shapiro-Wilk test was used to determine whether the data were normally distributed. A one-way or two-way ANOVA was used to indicate a significant difference as appropriate. Differences between groups were examined using multiple comparison test with Tukey correction for multiple comparisons. Data are shown as means ± SD. $P < 0.05$ was considered statistically significant in all tests.

Chapter Three: Results

3.1. Characterization of murine atherosclerotic model post-JUUL exposure

Wild-type mice do not develop atherosclerosis, even on a high-fat diet (117). Thus, in order to test whether JUUL exposure enhanced early pro-atherogenic changes, we utilized an inducible hyperlipidemic mouse model. C57BL/6 male mice were injected with AAV-PCSK9^{DY} virus at 4-weeks of age, and on the same day, were started a high fat diet. One week following injection, the mice were exposed to either room air, JUUL containing PG/VG solvent only or JUUL aerosol with mango flavour and 59 mg/ml nicotine (Fig.5A). Increased lipid levels are a blood biomarker for adequate AAV-PCSK9 expression and LDL-r knock-down. Hypercholesterolemia (with total cholesterol levels > 200 mg/dl) reflects appropriate AAV-PCSK9^{DY} function (160). Thus, plasma lipid levels were evaluated and only those mice with total cholesterol levels higher than 200 mg/dl (Fig. 5B) were further analyzed as reflection of appropriate AAV-PCSK9^{DY} function. Additionally, we measured the weight of mice before and after the experiment. After 4 weeks of exposure, we noticed significant increases in the weight of mice exposed to room air compared to day 0 of exposure ($P=0.005$; Fig. 1C), while the exposure in PG/VG and JUUL mango groups failed to gain weight (Fig. 1C). We have previously established this model of moderate JUUL exposure in C57BL/6 mice, based on the levels of the nicotine metabolite cotinine (34). Here, cotinine was measured 24 hours after the last exposure in all mice using ELISA. As expected, we found significant increases in cotinine level in the JUUL mango group compared to Air and PG/VG groups ($P<0.0001$; Fig.5E) with levels ranging between 10-40 ng/ml, although we did not observe changes in the hepatic CYP2A5 protein expression among exposure groups (Fig.5E).

A

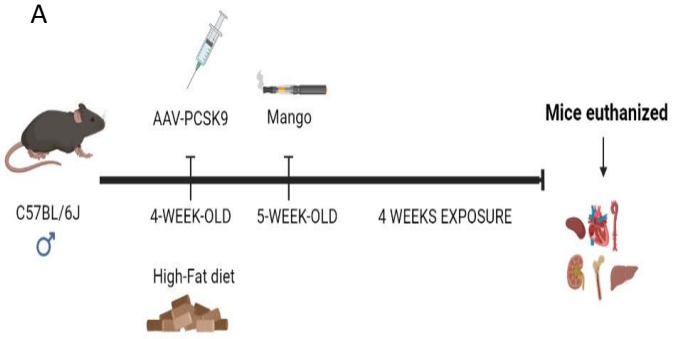
AAV-PCSK9
Mango
Mice euthanized
C57BL/6J
4-WEEK-OLD
5-WEEK-OLD
4 WEEKS EXPOSURE
High-Fat diet

B

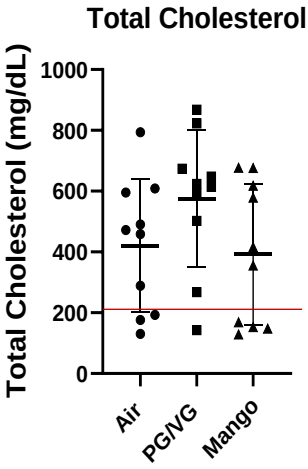
Total Cholesterol
Total Cholesterol (mg/dL)
1000
800
600
400
200
0
Air
PG/VG
Mango

C

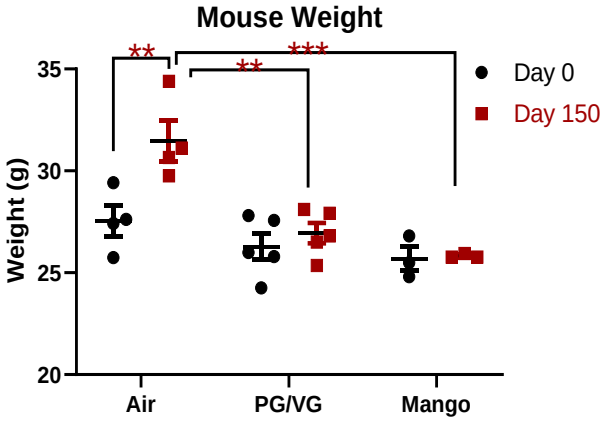
Mouse Weight
**
**
***
Day 0
Day 150
Weight (g)
35
30
25
20
Air
PG/VG
Mango

D

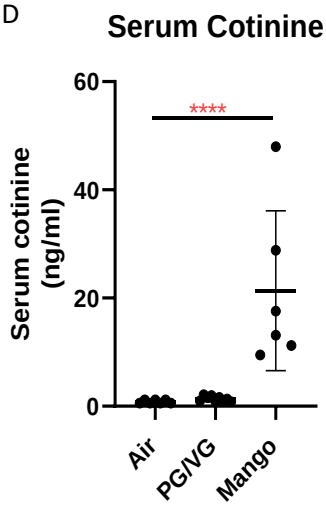
Serum Cotinine
Serum cotinine (ng/ml)
****
60
40
20
0
Air
PG/VG
Mango

E

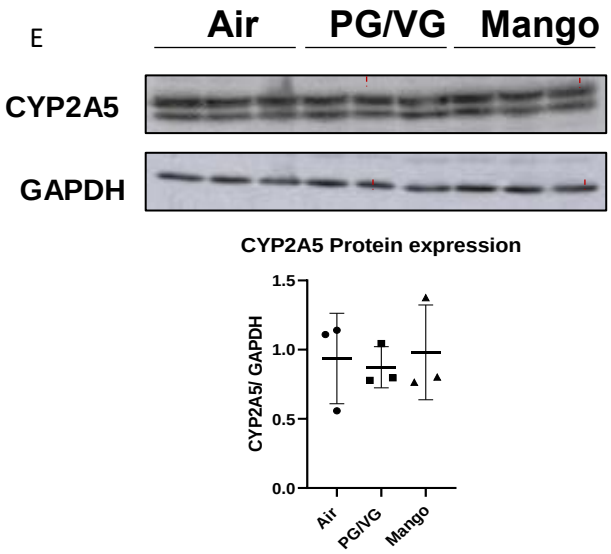
Air
PG/VG
Mango
CYP2A5
GAPDH
CYP2A5 Protein expression
CYP2A5/ GAPDH
1.5
1.0
0.5
0.0
Air
PG/VG
Mango

Fig.5. Exposure design and mouse model. **(A)** C57BL/6 male mice (N=10 per group) were injected with AAV-PCSK9 virus at 4-week of age, at the same day of injection mice were started on high fat diet. One week following injection mice were exposed to either room air, JUUL containing PG/VG solvent only or JUUL aerosol with mango flavour and 59 mg/ml nicotine. Mice were exposed to 4 puffs per min for 20 minutes 3times a day for 4 weeks. **(B)** Serum cholesterol level of mice injected with PCSK9 virus. Samples with total cholesterol level less than 200 mg/dl were excluded. **(C)** Mice weight were measured before and after the exposure**.** There was a remarkable but not significant gain of weight in air group but not JUUL groups after 4 weeks of exposure. **(D)** Serum cotinine level was measured by ELISA after 24hours of last exposure in hyperlipidemic mice. There was a significant increase in cotinine level in the JUUL mango group compared to Air and PG/VG groups ($P<0.0001$). **(E)** Liver was harvested at the end point. Later, protein was extracted, and Western Blot was performed to quantify the expression of CYP2A5. **(E)** CYP2A5 relative protein expression is shown no difference among exposure groups. Results are expressed as the mean ± SD; individual data points represent individual mice from two separate experiments (N= 6-9 per group).

3.2. Inhalation of JUUL aerosols in hyperlipidemic mice results in pro-atherogenic changes

Although at this early time point, the plaques were anticipated to be quite small, we evaluated the size and lipid content of the atherosclerotic plaques, (128). After oil red O staining, the percentage of plaque size per sinus area was calculated within the aortic sinus. As expected, the atherosclerotic plaques in all mice were small and no significant changes were observed between groups, although there was a trend of increased plaque size in the PG/VG group compared to the control group ($P=0.1$; Fig.6A). Moreover, the percentage of lipid content within plaque was not statistically different between groups, although the same trend of increased lipid content in the PG/VG-exposed group compared to the control group was observed (Fig. 6B).

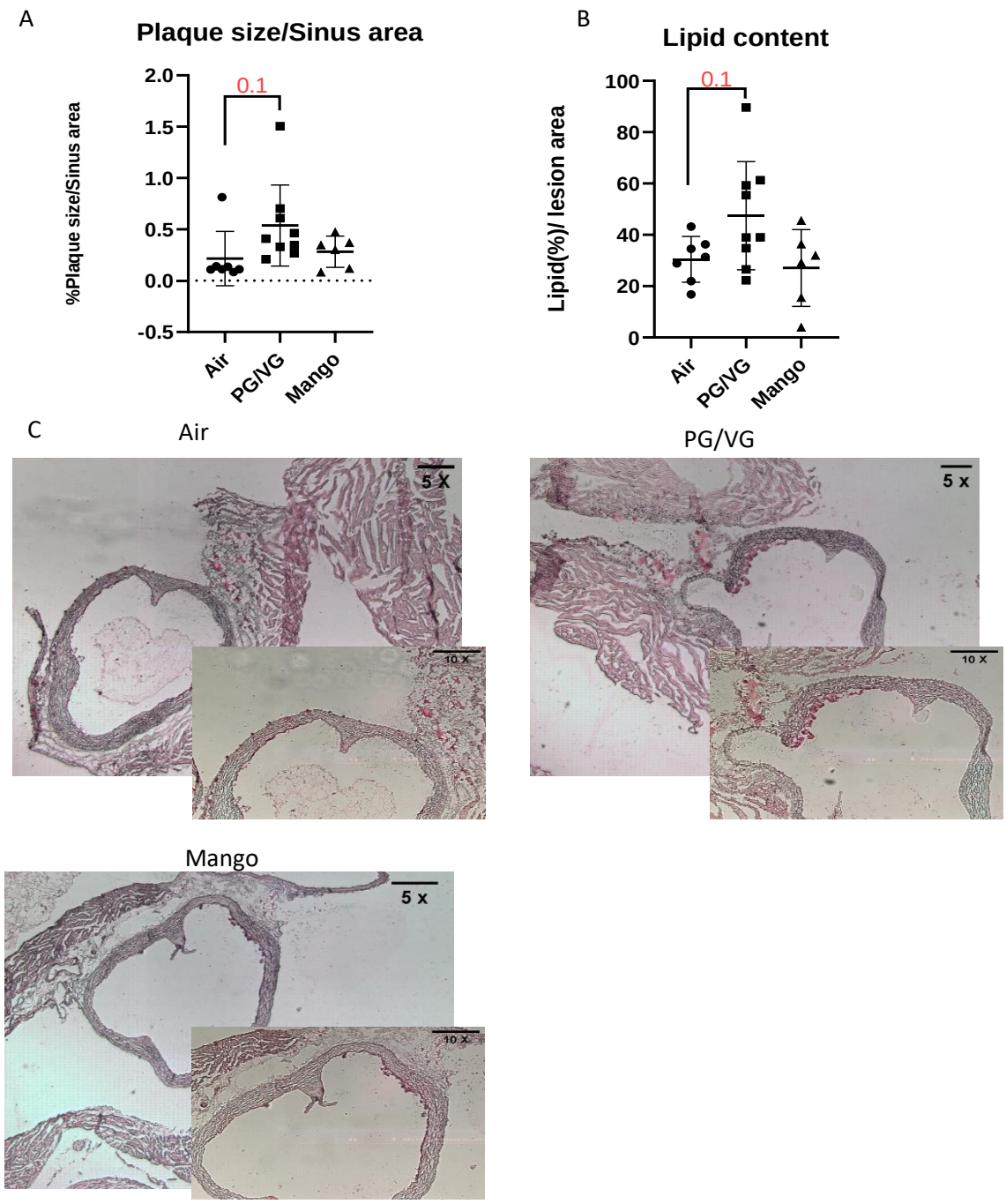

Fig.6. JUUL aerosol exposure tend to increase plaque formation and lipid deposition on aortic sinus in hyperlipidemic mice in nicotine-independent manner. Mice were exposed to air or JUUL aerosols with or without nicotine (4puffs/min) for four weeks. **(A)** Plaque size and **(B)** lipid content were quantified in the aortic sinus after oil red O staining and imaging. Representative images from each group are shown in(**C1-C3)**. Results are expressed as the mean ± SD; individual data points represent individual mice from two separate experiments(N= 6-9 per group).

Next, we evaluated earlier markers of vascular outcomes. First, we assessed soluble markers of endothelial cell activation (ICAM-1, PECAM-1, E-selectin, and P-selectin) in the serum, comparing AAV-PCSK9^{DY}-infected C57BL/6 mice exposed to air, PG/VG and JUUL mango with unexposed, uninfected wild-type mice. As expected, the levels of all markers were remarkably higher in the hyperlipidemic mice compared to wild type mice (Fig.7A-D). However, no changes were observed amongst exposure groups (Fig. 7A-D). In addition, we assessed VCAM-1 expression in the brachiocephalic arch (BCA) and carotid endothelial walls of the AAV-PCSK9^{DY}-infected mice using IHC. No significant differences were observed in either the in BCA (Fig.8A) or carotid tissues (Fig.8B).

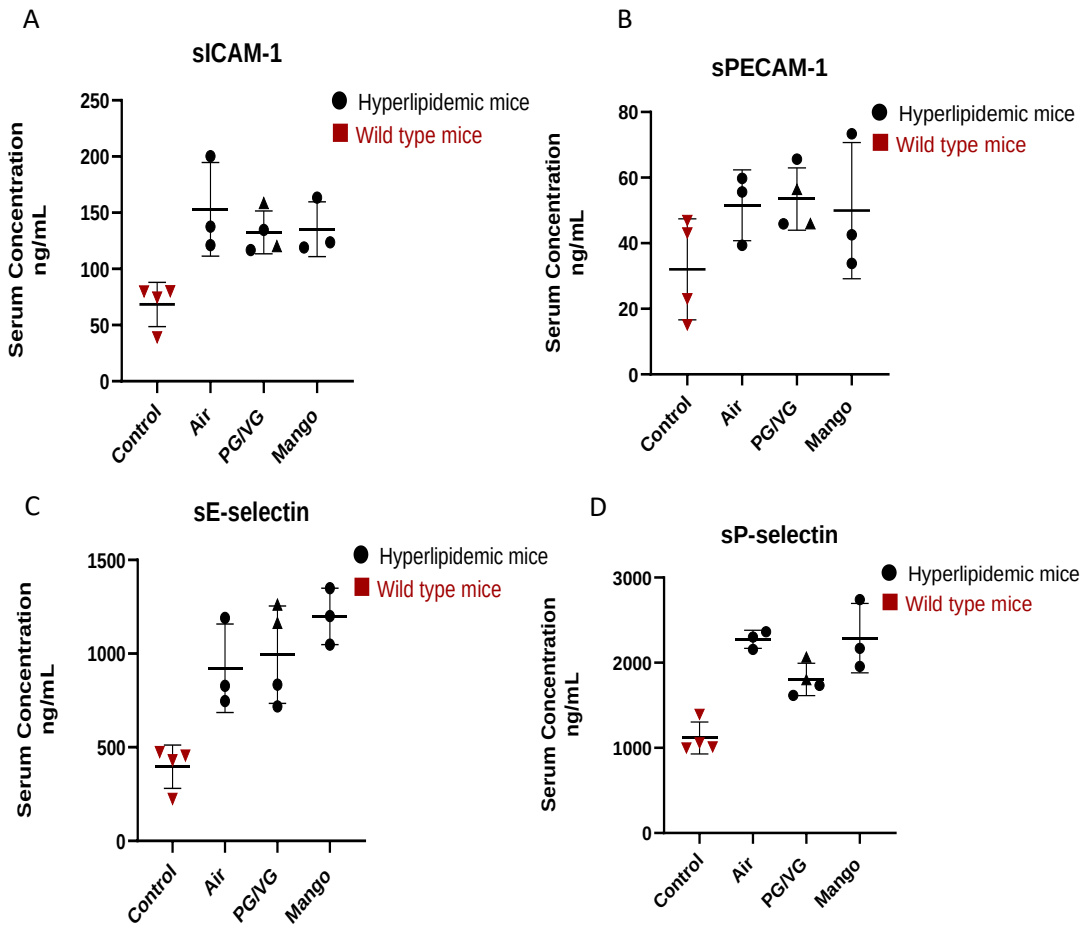

Fig.7. JUUL aerosol exposure in hyperlipidemic mice does result in a pattern of increase in some of the pro-atherogenic endothelial cell activation markers comparing with wild-type mice. Adhesion molecules **(A)** sICAM-1, **(B)** s-PECAM-1, **(C)** sE-selectin, and **(D)** sP-selectin were assessed in the serum of hyperlipidemic and wild type mice using CVD panel. Results are expressed as the mean ± SD; individual data points represent individual mice from two separate experiments(N= 3-4 per group).

A.1. Air

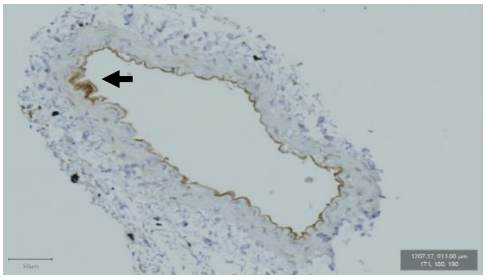

A.2.

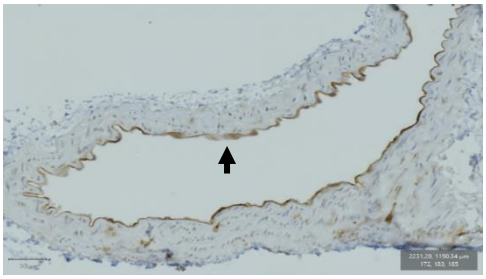

A.3.

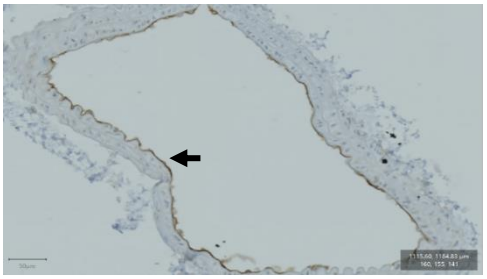

A.

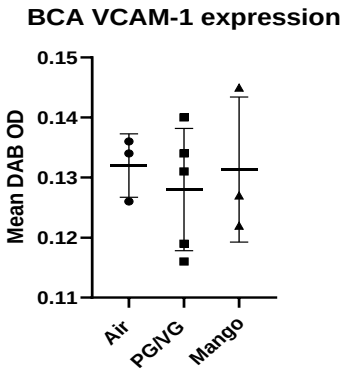

B.1. Air

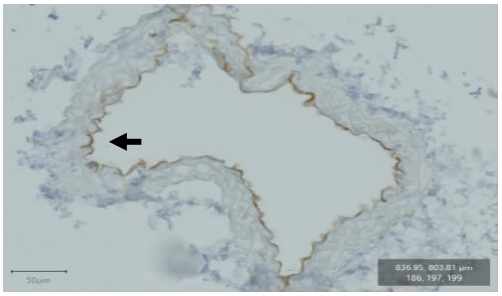

B.2. PG/VG

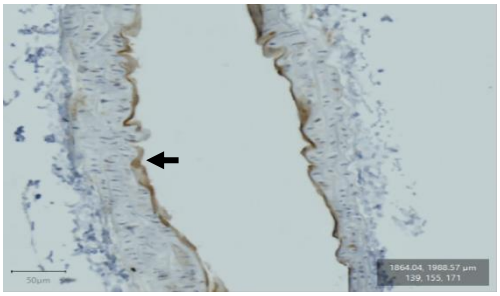

B.3.

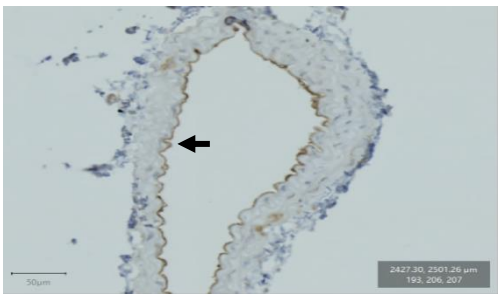

B.4

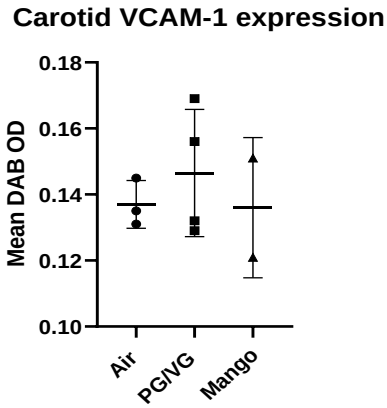

Fig.8. JUUL aerosol exposure show no effect on VCAM-1 expression in BCA and Carotid endothelial walls. VCAM-1 expression on the **(A)**BCA and **(B)** Carotid endothelial walls was evaluated using IHC staining and quantified by measuring Mean DAB OD. BCA representative images from each group are shown in **(A.1-A.4),** Carotid representative images from each group are shown in **(B.1-B.4).** . Results are expressed as the mean ± SD; individual data points represent individual mice from two separate experiments (N= 2-5 per group).

Finally, dyslipidemia is associated with atherosclerosis and is an early risk factor for CVD (161). We measured circulating triglyceride, LDL, HDL, and glucose levels. Significant decreases in both HDL and glucose levels were observed in the JUUL mango group compared to the control group ($P<0.05$; Fig. 9A,9B), while no changes were observed in triglyceride and LDL levels among exposure groups (Fig. 9C,9D).

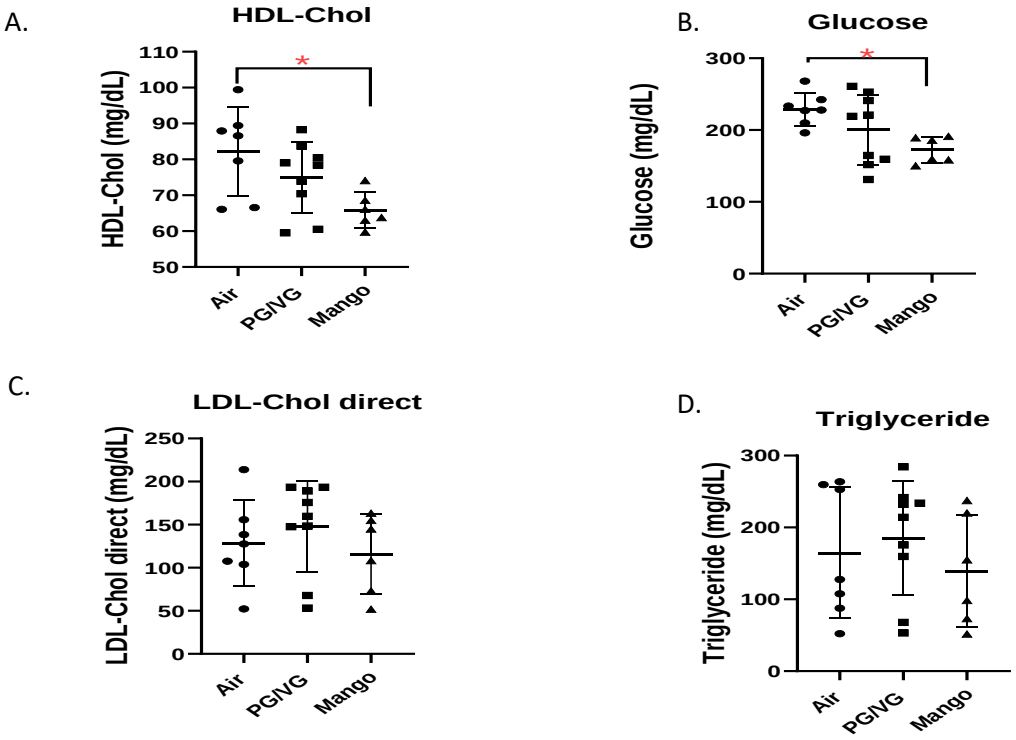

Fig.9. Serum lipid levels of mice injected with PCSK9 virus. **(A)**There was a significant decrease in HDL-Chol and **(B)** Glucose levels in the Mango group compared to control (*= $p<0.05$)**. (C,D)** Single PCSK9 virus injection resulted in increased lipid levels in all the exposure groups. Results are expressed as the mean ± SD; individual data points represent individual mice from two separate experiments (N= 6-9 per group).

3.3. *Inhalation of JUUL aerosols increases indices of systemic inflammation*

Given that atherosclerosis is caused by systemic inflammation, we sought to assess whether JUUL exposure would result in modulation of immune cells. To do so, we performed immunophenotyping on splenic cells, where we assessed lymphoid and myeloid lineages of immune cells. The percentage of total $CD3^+$ T cells was decreased in the JUUL Mango group compared to PG/VG ($P<0.05$; Fig. 10A). Furthermore, total $CD4^+$ cells and CD4+ Th cells were significantly decreased following JUUL mango exposure compared to both control and PG/VG groups ($P<0.05$, $P<0.005$; Fig. 10B,10C). On the other hand, the percentage of $CD4^+$ Tregs was not altered (Fig. 10D). Finally, the percentage of $CD8^+$ cytotoxic T cells in the PG/VG group was increased compared to the control ($P=0.05$; Fig.10E) and JUUL mango exposures groups ($P<0.05$; Fig.10E), although only statistically significant when compared to JUUL mango group. No significant changes were observed either in myeloid cell or B cell populations within the spleen (Fig.11A-G). Together, our data showed that vaping JUUL does cause changes in immune cell compositions increasing indices of systemic inflammation.

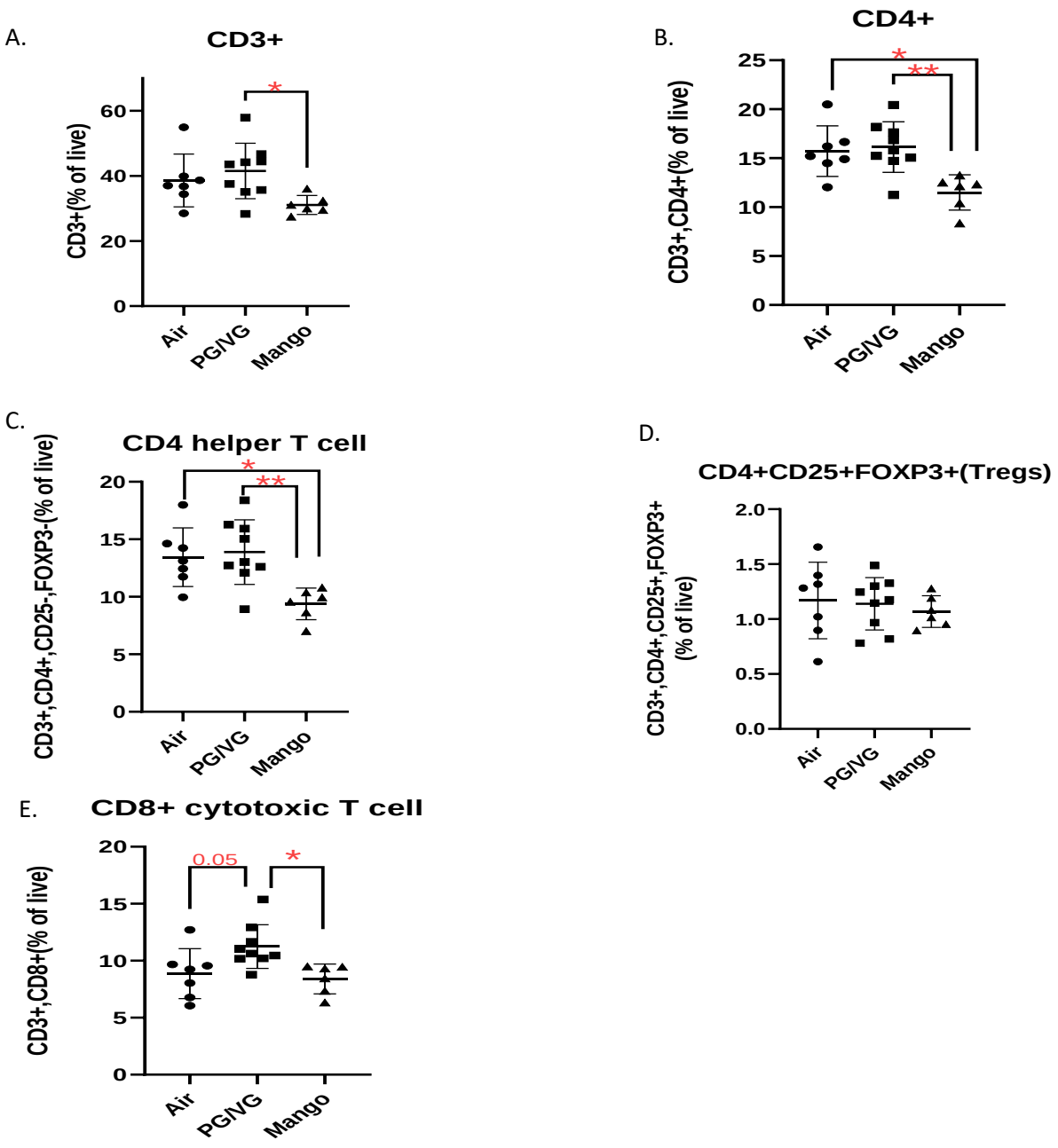

Fig.10. JUUL aerosol exposure does cause changes in immune cell compositions. Using immunophenotyping, lymphoid lineages of immune cells were assessed by performing Extended T-cell panel. Cell suspension of spleen were isolated from mice after 4 weeks exposure. The cells were stained with **(A)** CD3 antibody for total T-cells. **(B)** CD3 and CD4 antibodies for CD4+ T cells. **(C)** CD3, CD4, CD25 and FoxP3 antibodies for CD25- FoxP3- Th-cells and **(D)** CD25+ FoxP3+Tregs. **(E)** CD3 and CD8 antibodies for CD8+ T cells. The cells were then subjected to flow cytometry to determine cell-type percentages. Results are expressed as the mean ± SD; individual data points represent individual mice from two separate experiments(N= 6-9 per group). (*= $p<0.05$, **= $p<0.005$)

A.

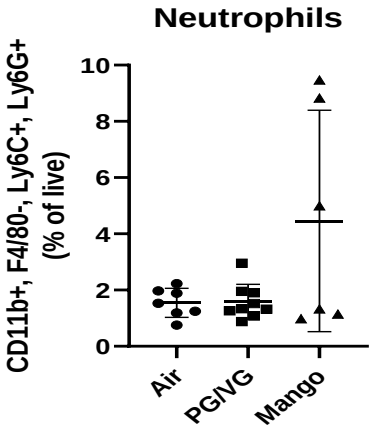
Neutrophils
CD11b+, F4/80-, Ly6C+, Ly6G+ (% of live)
10
8
6
4
2
0
Air
PG/VG
Mango

B.

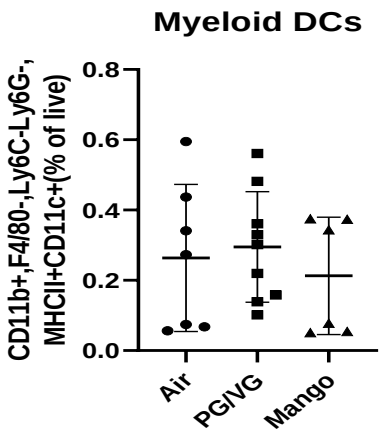
Myeloid DCs
CD11b+,F4/80-,Ly6C-Ly6G-, MHCII+CD11c+(% of live)
0.8
0.6
0.4
0.2
0.0
Air
PG/VG
Mango

C.

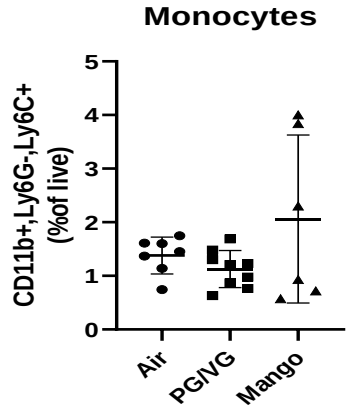
Monocytes
CD11b+,Ly6G-,Ly6C+ (%of live)
5
4
3
2
1
0
Air
PG/VG
Mango

D.

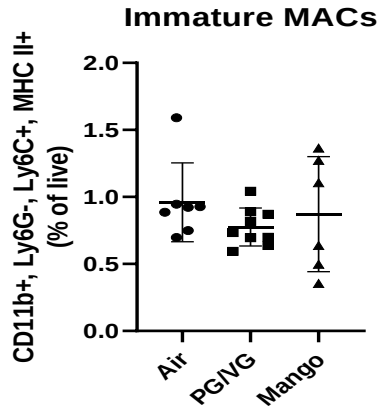
Immature MACs
CD11b+, Ly6G-, Ly6C+, MHC II+ (% of live)
2.0
1.5
1.0
0.5
0.0
Air
PG/VG
Mango

E.

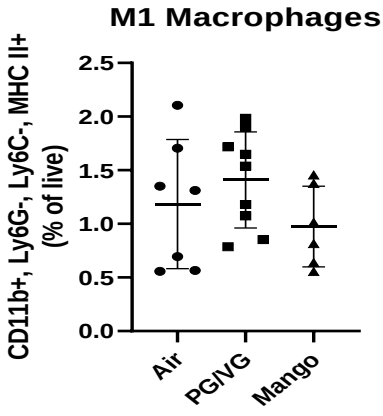
M1 Macrophages
CD11b+, Ly6G-, Ly6C-, MHC II+ (% of live)
2.5
2.0
1.5
1.0
0.5
0.0
Air
PG/VG
Mango

F.

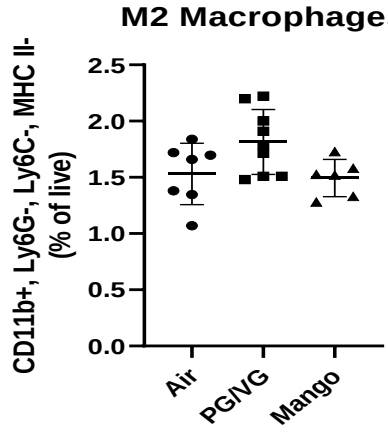
M2 Macrophages
CD11b+, Ly6G-, Ly6C-, MHC II- (% of live)
2.5
2.0
1.5
1.0
0.5
0.0
Air
PG/VG
Mango

G.

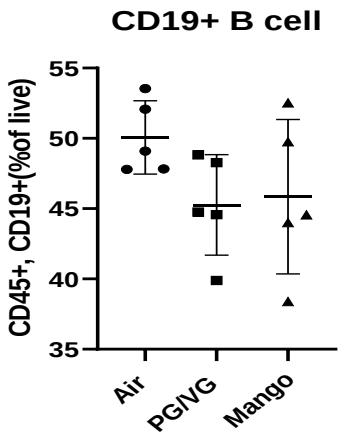
CD19+ B cell
CD45+, CD19+(%of live)
55
50
45
40
35
Air
PG/VG
Mango

Fig.11. Effect of JUUL aerosol exposure on immune cell distribution of myeloid cells and B cells. Using immunophenotyping, myeloid lineages of immune cells and B cells were assessed by performing myeloid panel. Cell suspension of spleen were isolated from mice after 4 weeks exposure. The cells were stained with **(A)** CD11b, Ly6C and Ly6G antibodies for neutrophils, **(B)** CD11b and CD11c antibodies for myeloid DCs, **(C)** CD11b and Ly6C antibodies for monocyte, **(D-F)** CD11b, Ly6G, Ly6C, and MHCII antibodies for immature, M1, and M2 macrophages, and **(G)** CD19 for B cells**.** The cells were then subjected to flow cytometry to determine cell-type percentages. Results are expressed as the mean ± SD; individual data points represent individual mice from two separate experiments (N= 6-9 per group).

Chapter Four: Discussion

The use of e-cigarettes has been associated to negative cardiovascular (162) and immunological responses (163, 164). Despite the surge in e-cigarette usage among teenagers, particularly the use of the JUUL brand, the health effects of JUUL use among never-smokers remain mostly unclear (2). Furthermore, the vascular consequences of e-cigarettes, particularly atherosclerosis, remain debatable (156, 157). In this study, our findings showed that the AAV-PCSK9 model is a working model for studying the pro-atherogenic effects of vaping JUUL in hyperlipidemic mice. Additionally, we showed that even a modest exposure (4 puffs per minute) for a relatively short length of time (4 weeks) is enough to observe early proatherogenic indicators.

The pathogenesis of atherosclerosis in humans and mice is a complicated process driven by a variety of risk factors such as ageing, hyperlipidemia, hypertension, and diabetes, which results in immunometabolic dysregulation (40). Thus, the investigation of the immunometabolic processes underlying atherosclerosis requires the use of animal models that replicate human pathophysiology. However, due to their drastically different lipid profile from humans, mice are highly resistant to the development of atherosclerosis (117, 118), therefore, genetic modification of their lipid metabolism is required. In this study, we used AAV-PCSK9^{DY}-infected C57BL/6 mice as our atherosclerotic model, and we used a single injection of recombinant adeno-associated virus (rAAV) encoding gain-of-function mutant forms of PCSK9. A single injection is known to be sufficient to cause downregulation of LDLr inducing hyperlipidemia and atherosclerosis in mice, where plaque formation is similar to what is found in humans (123, 150). Using this model allowed us to control the time of atherosclerosis induction to evaluate the

impact of JUUL in various scenarios that mimic human outcomes. Establishing this exposure model was a first step toward developing these unique exposure scenarios. For instance, in the future, we can test if excessive JUUL use in adolescence predisposes them to cardiovascular risk later in life, where bad lifestyle choices, such as a high fat diet and smoking, combine to raise the risk. Using this model will allow us to start an exposure in which young mice are only exposed to JUUL for 8 weeks before being injected with AAV-PCSK9 to induce hyperlipidemia (with and without a high fat diet) and see whether there are any variations in cardiopulmonary outcomes. Furthermore, we can explore whether switching from cigarette smoking to JUUL (in conjunction with the AAV-PCKS9) reduces cardiovascular risk and reduces pulmonary and systemic inflammation.

To ensure that our exposure correlated with human exposure, in addition to our designed puff topography (i.e., puff volume, puff interval, etc.), we tested cotinine levels in the blood. We chose cotinine over nicotine to be assessed since it has a longer half-life in vivo ($t_{1/2} \approx 7$ minutes for nicotine vs ≈ 40 minutes for cotinine) (165). We found blood cotinine level (10-40 ng/ml) to be lower than what was found in the saliva (122 ng/ml) in a study conducted on human JUUL users (pods containing 5% nicotine) (166). However, we are comparing blood to saliva, and while cotinine levels in blood and saliva are substantially related, saliva levels are typically 15-20% greater than plasma levels (167). In addition, this discrepancy corresponded to the kinetics of cotinine metabolism, which is faster in mice than in humans ($t_{1/2} = 2$ hours for nicotine vs 16-18 hours for cotinine in humans) (16, 165). Furthermore, the time course of cotinine in the body and the resulting pharmacologic effects are highly dependent on species, dose, route, and rate of dosing (16). With these considerations in mind, the exposure is most likely comparable to what is observed in humans.

Dyslipidemia is associated with atherosclerosis and is an early risk factor for CVD (161), thus we measured triglyceride, LDL, HDL, and glucose levels. We observed a significant decrease in HDL levels in the JUUL mango group compared to the control group. Curiously, another study conducted on $Apoe^{-/-}$ mice, funded by a tobacco company, found no changes in HDL levels after three- and six-months of exposure to e- cigarette aerosols containing PG/VG, 4% nicotine, and flavor mix (157). Despite the differences between their exposure (i.e., full body exposure system, longer exposure time, and different strain) and our exposure, our finding of just after 4 weeks of exposure is concerning, given that HDL plays an important role in the clearance of cholesterol from tissues (168). In addition, HDL maintains plaque stability by inhibiting degradation of the fibrous cap extracellular matrix through its anti-elastase activity (169). Thus, decreased HDL levels could imply that JUUL mango results in insufficient clearance of cholesterol from tissues, causing excess cholesterol to accumulate in the arteries, thus increasing the risk of atherosclerosis. Ultimately, exposure to JUUL flavored mango for a prolong period of time, could contribute to decreased plaque stability resulting in plaque prone to rupture.

Furthermore, when comparing the JUUL mango group to the control group, we saw a substantial drop in glucose levels. This discovery contrast with findings of a population study that found nicotine from tobacco smoking caused increases in blood glucose concentrations (170). Furthermore, a study published in 2022, discovered that e-cigarette usage resulted in elevated glucose levels in humans, which led to a higher risk of prediabetes (171). The discrepancies in these results may be due to several factors, including species, brand of e-cigarettes used, addition of flavoring, the dose of nicotine, and the hyperlipidemic profile.

Interestingly, after 4 weeks of JUUL exposure and high-fat diet consumption, we observed significant increases in the weight of mice exposed to room air, but mice exposed to PG/VG or JUUL mango failed to gain weight. Our findings are consistent with a previous report on the effect of short (2 weeks) e-cigarette exposure on cardiac function and body weight in C57BL/6 mice, where they found that e-cigarette vaping significantly inhibited the bodyweight gain (172). Moreover, our findings are similar to what was observed early (4 weeks) in $Apoe^{-/-}$ mice exposed to e-cigarette aerosols and fed high fat-diet for 12 weeks, although the decrease in weight was only observed in the nicotine (2.4%) group (156). However, considering their data, the change in weight maybe transient, suggesting that the weight of mice exposed to JUUL products may alter over a longer duration of exposure. Because the purpose of our experimental design was not to evaluate bodyweight change, we did not quantify food and water intake in these animals. We also did not measure any metabolic markers for weight increase, such as leptin and peroxisome proliferator-activated receptors (PPARs). Leptin is a hormone largely generated in adipose cells that controls food intake, metabolic rate, and body weight. It is hypothesized to assist weight reduction by decreasing hunger and boosting metabolism in rats (173). PPARs are ligand-activated transcription factors that are activated by endogenous ligands obtained from the metabolism of fatty acids and other dietary components (174). This is in accordance with the fact that PPARs govern the expression of several genes involved in glucose and lipid metabolism. As a result, it is unclear whether the effect of e-cigarettes on bodyweight gain is due to reduced food consumption (supressed appetite) or other processes. More research is needed to determine the specific processes or explanations of weight maintenance in mice exposed to JUUL products.

To our knowledge, ours is the first study using the PCSK9 mouse model to study the effects of JUUL products on atherosclerotic outcomes. First, we measured the size and lipid content of the atherosclerotic plaques, which were expected to be fairly tiny at this early stage (128) . A previous study demonstrated that Apoe$^{-/-}$ mice exposed to vaping a nicotine-containing product and fed a high fat diet for 12 weeks resulted in a striking increase in plaque size ($P < 0.01$) (156). On the other hand, another study (funded by a tobacco company) showed no significant difference in plaque size after 3 and 6 months of vaping exposure compared to the control group (157). In our study, we found that simply 4 weeks of JUUL use did not significantly enhance plaque size or lipid content, although there was a trend of increased plaque size and lipid content in the PG/VG group when compared to the control group. The comparison of our findings to earlier studies is complicated by the different exposure regimens and device/e-liquids used. This was clearly manifested in our prior work, where we saw varied results by varying the exposure regimes (1 puff vs 4 puffs) and utilising various e-liquid components (i.e., flavours), despite the fact that we utilised the same device (JUUL) (34). Our data however suggests that the possible effect of JUUL aerosols on plaque size and lipid content is highly dependent on the presence/ absence of some of the e-liquid components (e.g., PG/VG, nicotine, and flavour).

In atherogenesis, in hyperlipidemic mice (Apoe$^{-/-}$mice) fed western diets, the attachment of monocyte to endothelial cells was observed after 6 weeks (128). Then, a time course of 8 weeks was required to observe the fatty streak seen in the early stages of atherosclerosis, a net product of macrophage conversion into foam cells (43, 128). Where after 15-20 weeks, intermediate lesions were detected composing of SMCs, extracellular matrix and a necrotic core covered with a fibrous cap. Thus, whereas our data showed short JUUL exposure (4 weeks) in conjunction with hyperlipidemic condition resulted in tiny plaques with no significant differences between

groups, extended exposure (i.e., 12 weeks or 6 months) may result in a considerable increase in plaque size.

Next, we evaluated earlier markers of vascular outcomes. First, we assessed soluble markers of endothelial cell activation: ICAM-1, PECAM-1, E-selectin, and P-selectin levels in the serum. Secondly, we assessed VCAM-1 expression in the brachiocephalic arch (BCA) and carotid endothelial walls. Soluble adhesion molecule levels have been linked to a variety of cardiovascular risk factors, including smoking (61), hypertension (62), low HDL cholesterol (63), and hypercholesterolemia and/or hypertriglyceridemia (64, 65). Soluble adhesion molecules have been postulated as an index for the degree and severity of atherosclerosis. VCAM-1 plays an important role in the firm adhesion between monocyte and ECs (26). In addition, elevated levels of VCAM-1 enhance macrophage proliferation, resulting in a high number of macrophages aggregating in the plaque, thus enhancing plaque instability (51). In our study, we found that a 4-week exposure to JUUL aerosols caused no changes in the soluble adhesion molecule levels and resulted in no significant differences in VCAM-1 expression in either the BCA or carotid tissues. Occurrence of high adhesion molecule levels were mainly reported after long stimuli exposure, although elevated levels are observed early in pathogenesis (66-68).

We found by immunoprofiling that PG/VG and JUUL exposure altered specific splenic immune cell populations. The spleen, being the largest lymph node, is the primary filter for blood-borne infections and antigens, and because more cells pass through the spleen than through all other secondary lymphoid organs combined, its contribution to cell recirculation is critical (175, 176). All of which, in addition to its importance in controlling systemic immunity, the spleen was chosen as the target organ, despite the fact that its lymphoid and myeloid populations do not represent what may be seen inside the plaque (175). Our findings support the

notion that JUUL has a remarkable impact on adaptive cells in the spleen. In this study, mango-flavored JUUL significantly decreased CD3+ and CD4+ T cells. This indicates the presence of interference in the immune response, as CD4 T cells play a central role in immune protection through their capacity to help B cells make antibodies, to induce macrophages to develop enhanced microbicidal activity, and to recruit granulocytes to sites of infection and inflammation (177). In addition, $CD4^+$ T cells can be found in the atherosclerotic plaque where they release Th1-associated pro-inflammatory cytokines, such as IL-2, IL-3, TNF-α, and lymphotoxin, all of which can activate macrophages, T cells, and other plaque cells resulting in acceleration of the inflammatory response (100). Thus, impaired CD4+ T cell function in the spleen may increase infection susceptibility and might play an indirect role in the absence of plaque size growth found in the JUUL mango group. Unlike T cells, myeloid lineage cells such as neutrophils, monocytes, and macrophages, as well as B cells, did not change after vaping. Together, our findings suggest that vaping JUUL produces changes in immune cell composition, which could interfere with the host defence mechanism. Further studies could be conducted to deeply investigate T cells functionality after JUUL vaping to better understand such observations. For instance, T cell activation markers (i.e., CD134 and Inducible costimulatory molecule) and inhibition markers (i.e., CD210 and programmed death-1) could be evaluated by immunophenotyping as a straightforward approach. In addition, proliferation of T cells and the amount of INF-γ secreted could be tested using proliferation assay (178). Another approach would be isolating the peripheral blood mononuclear cells (PBMCs) then performing IFN-γ ELISpot assay to test the immune response after vaping (179).

Although many of the substances in e-liquids are 'Generally Recognized as Safe' for oral intake (e.g., PG/VG and flavours), there is little data on their safety when aerosolized and inhaled (23). Unexpectedly, our data revealed some alterations observed exclusively in the PG/VG group. Previous findings reported a decrease in mice weight exposed to vaping aerosol containing nicotine (156, 172). Nicotine is known to play a role in appetite suppression thus decreasing / inhibiting bodyweight (180), however, in our findings, suppressed weight gain was observed also in the PG/VG group. Moreover, our findings from plaque size and CD8+ T cell population, showed a trend of increase in PG/VG group alone. This increase was suppressed in mango-flavored JUUL possibly due to the presence of nicotine, the flavoring, or both. Although, we only detected a trend of increase at this early time point, it might be exacerbated later with prolonged exposure. Together, our findings suggest that PG/VG is not inert and however, these mice were not just exposed to PG/VG. Another important factor is the metal coil, which is often constructed of nichrome (a mix of Ni and Cr) and stainless steel. Toxic metals from heated coils have previously been shown to leak into e-liquids and ultimately into vaping aerosols (7). A study revealed that coil contact produced e-liquid contamination, meaning that e-cigarettes might be a source of harmful metal exposure such as Cr and Ni (22). This was demonstrated by a study that discovered a link between increased e-cigarette usage and consumption and higher Ni and Cr biomarker concentrations (21). As such, metals can not be ruled out as a synergistic factor in the case of PG/VG, or as an inhibitor factor in the context of mango flavored JUUL.

4.1.Limitations

Our study's strengths include the use of a distinctive e-cigarette delivery method that mimics human vaping and the use of a leading brand of e-cigarettes that produced serum cotinine levels in the range reported in moderate smokers; nonetheless, our study has several drawbacks. The use of just male mice, the period of exposure, and the small sample size in this study might all be considered limitations. Because our study was done on male mice, the results may not be generalized for females. We only investigated the impact of daily JUUL aerosol inhalation for four weeks and it might be possible that other/worse effects would be observed with longer-term exposures. While individuals use e-cigarettes throughout the day, repeatedly pulling out their e-device and vaping, this usage pattern was not adequately replicated in our study where the exposures were done three times daily. However, this time constraint of 20 minutes, three times per day, was required to provide mice access to food and water while keeping their stress levels to a minimum. Any future research might be hampered by the fact that the mango JUUL flavour does not reflect any other flavors. However, it was made up of compounds that are often present in other flavours, therefore these findings could be applicable to other vapes. Finally, the manufacturing and design of e-cigarettes appear to be constantly evolving, making it difficult to rigorously and systematically investigate the devices while keeping up with the constant advancements; we began this study with JUUL being the dominant brand in the market, but this is no longer the case. To address the rapid surge in JUUL usage among teens, Health Canada has set limitations on some e-cigarette flavours, limiting them to tobacco and mint/menthol. In fact, the newest FDA investigations discovered that JUUL purposefully promoted its products to adolescents, despite the fact that e-cigarette sales to children are illegal. As a result of the present settlement, JUUL's sales and marketing capabilities will be limited, including prohibitions on

marketing to individuals under the age of 35, limits on in-store displays, online and retail sales limits, and a retail compliance check methodology. The latest regulations resulted in an increase in the usage of disposable e-cigarettes (such as Puff Bar™) since they are available in flavours that were previously prohibited in pod-based e-cigarettes (JUUL) (181). This adds to the difficulty of evaluating the health effects of different devices (pod-based versus disposable e-cigarette devices) and hence establishing regulations. E-cigarette device and liquid combinations that yield a higher nicotine emission rate (i.e., higher nicotine flux) result in increased e-cigarette dependency. Preliminary research revealed that pod-based e-cigarettes had lower nicotine flux and concentration when compared to disposable e-cigarettes (182). Because e-cigarette devices and liquid properties are linked to nicotine dependency, the constant change of the e-cigarette landscape makes drawing health consequence conclusions problematic.

4.2. Conclusion

In conclusion, our results demonstrate that JUUL products are not harmless. In fact, JUUL exposure can induce early pro-atherogenic alterations in young hyperlipidemic mice, suggesting there could be increased cardiovascular disease later in life. These findings are alarming as e-cigarettes gain massive popularity among nonsmokers in teens and young adults. Appropriate awareness is demanded not only regarding the harmful effects of e-cigarettes (even without nicotine), but also regarding the implications of poor lifestyle choices early in life including consumption of high fat diets. Finally, these findings, combined with the constant evolution of e-cigarettes, highlight the significance of further studies on the effects of e-cigarettes from various devices containing different flavours.

References:

1. Caponnetto P, Campagna D, Papale G, Russo C, Polosa R. The emerging phenomenon of electronic cigarettes. Expert Rev Respir Med. 2012;6(1):63-74.

2. Civiletto CW, Hutchison J. Electronic Vaping Delivery Of Cannabis And Nicotine. StatPearls. Treasure Island (FL): StatPearls Publishing

3. Cahn Z, Siegel M. Electronic cigarettes as a harm reduction strategy for tobacco control: a step forward or a repeat of past mistakes? J Public Health Policy. 2011;32(1):16-31.

4. Fadus MC, Smith TT, Squeglia LM. The rise of e-cigarettes, pod mod devices, and JUUL among youth: Factors influencing use, health implications, and downstream effects. Drug Alcohol Depend. 2019;201:85-93.

5. O'Connell G, Pritchard JD, Prue C, Thompson J, Verron T, Graff D, et al. A randomised, open-label, cross-over clinical study to evaluate the pharmacokinetic profiles of cigarettes and e-cigarettes with nicotine salt formulations in US adult smokers. Intern Emerg Med. 2019;14(6):853-61.

6. Polosa R, Caponnetto P, Morjaria JB, Papale G, Campagna D, Russo C. Effect of an electronic nicotine delivery device (e-Cigarette) on smoking reduction and cessation: a prospective 6-month pilot study. BMC Public Health. 2011;11:786.

7. Traboulsi H, Cherian M, Abou Rjeili M, Preteroti M, Bourbeau J, Smith BM, et al. Inhalation Toxicology of Vaping Products and Implications for Pulmonary Health. Int J Mol Sci. 2020;21(10).

8. King BA, Gammon DG, Marynak KL, Rogers T. Electronic Cigarette Sales in the United States, 2013-2017. Jama. 2018;320(13):1379-80.

9. Jackler RK, Ramamurthi D. Nicotine arms race: JUUL and the high-nicotine product market. Tob Control. 2019;28(6):623-8.

10. Willett JG, Bennett M, Hair EC, Xiao H, Greenberg MS, Harvey E, et al. Recognition, use and perceptions of JUUL among youth and young adults. Tob Control. 2019;28(1):115-6.

11. Rouabhia M. Impact of Electronic Cigarettes on Oral Health: a Review. J Can Dent Assoc. 2020;86:k7.

12. Muthumalage T, Lamb T, Friedman MR, Rahman I. E-cigarette flavored pods induce inflammation, epithelial barrier dysfunction, and DNA damage in lung epithelial cells and monocytes. Scientific reports. 2019;9(1):1-11.

13. Goniewicz ML, Boykan R, Messina CR, Eliscu A, Tolentino J. High exposure to nicotine among adolescents who use Juul and other vape pod systems ('pods'). Tobacco control. 2019;28(6):676-7.

14. Pankow JF, Kim K, McWhirter KJ, Luo W, Escobedo JO, Strongin RM, et al. Benzene formation in electronic cigarettes. PloS one. 2017;12(3):e0173055.

15. Rao P, Liu J, Springer ML. JUUL and combusted cigarettes comparably impair endothelial function. Tobacco regulatory science. 2020;6(1):30-7.

16. Schick SF, Blount BC, Jacob PR, Saliba NA, Bernert JT, El Hellani A, et al. Biomarkers of exposure to new and emerging tobacco delivery products. Am J Physiol Lung Cell Mol Physiol. 2017;313(3):L425-l52.

17. Zhou X, Zhuo X, Xie F, Kluetzman K, Shu YZ, Humphreys WG, et al. Role of CYP2A5 in the clearance of nicotine and cotinine: insights from studies on a Cyp2a5-null mouse model. J Pharmacol Exp Ther. 2010;332(2):578-87.

18. Behar RZ, Hua M, Talbot P. Puffing topography and nicotine intake of electronic cigarette users. PLoS One. 2015;10(2):e0117222.

19. Marsot A, Simon N. Nicotine and Cotinine Levels With Electronic Cigarette: A Review. Int J Toxicol. 2016;35(2):179-85.

20. Shiplo S, Czoli CD, Hammond D. E-cigarette use in Canada: prevalence and patterns of use in a regulated market. BMJ open. 2015;5(8):e007971.

21. Aherrera A, Olmedo P, Grau-Perez M, Tanda S, Goessler W, Jarmul S, et al. The association of e-cigarette use with exposure to nickel and chromium: A preliminary study of non-invasive biomarkers. Environ Res. 2017;159:313-20.

22. Olmedo P, Goessler W, Tanda S, Grau-Perez M, Jarmul S, Aherrera A, et al. Metal Concentrations in e-Cigarette Liquid and Aerosol Samples: The Contribution of Metallic Coils. Environ Health Perspect. 2018;126(2):027010.

23. Kaur G, Muthumalage T, Rahman I. Mechanisms of toxicity and biomarkers of flavoring and flavor enhancing chemicals in emerging tobacco and non-tobacco products. Toxicology letters. 2018;288:143-55.

24. Schier JG, Meiman JG, Layden J, Mikosz CA, VanFrank B, King BA, et al. Severe pulmonary disease associated with electronic-cigarette–product use—interim guidance. Morbidity and Mortality Weekly Report. 2019;68(36):787.

25. Davidson K, Brancato A, Heetderks P, Mansour W, Matheis E, Nario M, et al. Outbreak of electronic-cigarette–associated acute lipoid pneumonia—North Carolina, July–August 2019. Morbidity and Mortality Weekly Report. 2019;68(36):784.

26. Xu H, Jiang J, Chen W, Li W, Chen Z. Vascular macrophages in atherosclerosis. Journal of immunology research. 2019;2019.

27. Blount BC, Karwowski MP, Shields PG, Morel-Espinosa M, Valentin-Blasini L, Gardner M, et al. Vitamin E acetate in bronchoalveolar-lavage fluid associated with EVALI. New England Journal of Medicine. 2020;382(8):697-705.

28. Pinkston R, Zaman H, Hossain E, Penn AL, Noël A. Cell-specific toxicity of short-term JUUL aerosol exposure to human bronchial epithelial cells and murine macrophages exposed at the air–liquid interface. Respiratory research. 2020;21(1):1-15.

29. Ramirez JEM, Karim ZA, Alarabi AB, Hernandez KR, Taleb ZB, Rivera JO, et al. The JUUL e-cigarette elevates the risk of thrombosis and potentiates platelet activation. Journal of Cardiovascular Pharmacology and Therapeutics. 2020;25(6):578-86.

30. Pearce K, Gray N, Gaur P, Jeon J, Suarez A, Shannahan J, et al. Toxicological analysis of aerosols derived from three electronic nicotine delivery systems using normal human bronchial epithelial cells. Toxicology in Vitro. 2020;69:104997.

31. O'Farrell HE, Brown R, Brown Z, Milijevic B, Ristovski ZD, Bowman RV, et al. E-cigarettes induce toxicity comparable to tobacco cigarettes in airway epithelium from patients with COPD. Toxicology in Vitro. 2021;75:105204.

32. Ghosh A, Beyazcicek O, Davis ES, Onyenwoke RU, Tarran R. Cellular effects of nicotine salt-containing e-liquids. Journal of Applied Toxicology. 2021;41(3):493-505.

33. Lamb T, Muthumalage T, Rahman I. Pod-based menthol and tobacco flavored e-cigarettes cause mitochondrial dysfunction in lung epithelial cells. Toxicology letters. 2020;333:303-11.

34. Been T, Traboulsi H, Paoli S, Alakhtar B, Mann KK, Eidelman DH, et al. Differential impact of JUUL flavors on pulmonary immune modulation and oxidative stress responses in male and female mice. Archives of Toxicology. 2022;96(6):1783-98.

35. Moshensky A, Brand C, Alhaddad H, Shin J, Masso-Silva JA, Advani I, et al. Effect of chronic JUUL aerosol inhalation on inflammatory states of the brain, lung, heart and colon in mice. bioRxiv. 2021.

36. Crotty Alexander LE, Drummond CA, Hepokoski M, Mathew D, Moshensky A, Willeford A, et al. Chronic inhalation of e-cigarette vapor containing nicotine disrupts airway barrier function and induces systemic inflammation and multiorgan fibrosis in mice. American Journal of Physiology-Regulatory, Integrative and Comparative Physiology. 2018;314(6):R834-R47.

37. Cirillo S, Vivarelli F, Turrini E, Fimognari C, Burattini S, Falcieri E, et al. The customizable e-cigarette resistance influences toxicological outcomes: Lung degeneration, inflammation, and oxidative stress-induced in a rat model. Toxicological Sciences. 2019;172(1):132-45.

38. Roth GA, Mensah GA, Johnson CO, Addolorato G, Ammirati E, Baddour LM, et al. Global burden of cardiovascular diseases and risk factors, 1990–2019: update from the GBD 2019 study. Journal of the American College of Cardiology. 2020;76(25):2982-3021.

39. Lu L, Liu M, Sun R, Zheng Y, Zhang P. Myocardial infarction: symptoms and treatments. Cell biochemistry and biophysics. 2015;72(3):865-7.

40. Falk E. Pathogenesis of atherosclerosis. Journal of the American College of cardiology. 2006;47(8S):C7-C12.

41. Turunen MP, Hiltunen MO, Ylä-Herttuala S. Gene therapy for angiogenesis, restenosis and related diseases. Experimental gerontology. 1999;34(4):567-74.

42. Gerrity RG. The role of the monocyte in atherogenesis: II. Migration of foam cells from atherosclerotic lesions. Am J Pathol. 1981;103(2):191-200.

43. Maguire EM, Pearce SWA, Xiao Q. Foam cell formation: A new target for fighting atherosclerosis and cardiovascular disease. Vascul Pharmacol. 2019;112:54-71.

44. STEPTOE A, BRYDON L. Psychosocial factors and coronary heart disease: the role of psychoneuroimmunological processes. Psychoneuroimmunology: Elsevier; 2007. p. 945-74.

45. Luttun A, Lutgens E, Manderveld A, Maris K, Collen D, Carmeliet P, et al. Loss of matrix metalloproteinase-9 or matrix metalloproteinase-12 protects apolipoprotein E–deficient mice against atherosclerotic media destruction but differentially affects plaque growth. Circulation. 2004;109(11):1408-14.

46. Daskalopoulos EP, Hermans KC, van Delft L, Altara R, Blankesteijn WM. The role of inflammation in myocardial infarction. Inflammation in Heart Failure: Elsevier; 2015. p. 39-65.

47. Katz S, Shipley GG, Small D. Physical chemistry of the lipids of human atherosclerotic lesions. Demonstration of a lesion intermediate between fatty streaks and advanced plaques. The Journal of clinical investigation. 1976;58(1):200-11.

48. Chistiakov DA, Melnichenko AA, Grechko AV, Myasoedova VA, Orekhov AN. Potential of anti-inflammatory agents for treatment of atherosclerosis. Experimental and Molecular Pathology. 2018;104(2):114-24.

49. Ranjit N, Diez-Roux AV, Shea S, Cushman M, Seeman T, Jackson SA, et al. Psychosocial factors and inflammation in the multi-ethnic study of atherosclerosis. Archives of Internal Medicine. 2007;167(2):174-81.

50. Zhu Y, Xian X, Wang Z, Bi Y, Chen Q, Han X, et al. Research Progress on the Relationship between Atherosclerosis and Inflammation. Biomolecules. 2018;8(3).

51. Mantovani A, Garlanda C, Locati M. Macrophage diversity and polarization in atherosclerosis: a question of balance. Arterioscler Thromb Vasc Biol. 2009;29(10):1419-23.

52. Goldberger A, Middleton KA, Oliver JA, Paddock C, Yan HC, DeLisser HM, et al. Biosynthesis and processing of the cell adhesion molecule PECAM-1 includes production of a soluble form. J Biol Chem. 1994;269(25):17183-91.

53. Blann AD, Nadar SK, Lip GY. The adhesion molecule P-selectin and cardiovascular disease. European heart journal. 2003;24(24):2166-79.

54. Blankenberg S, Barbaux S, Tiret L. Adhesion molecules and atherosclerosis. Atherosclerosis. 2003;170(2):191-203.

55. Galkina E, Ley K. Vascular adhesion molecules in atherosclerosis. Arterioscler Thromb Vasc Biol. 2007;27(11):2292-301.

56. Dong ZM, Chapman SM, Brown AA, Frenette PS, Hynes RO, Wagner DD. The combined role of P- and E-selectins in atherosclerosis. J Clin Invest. 1998;102(1):145-52.

57. Pasquali A, Trabetti E, Romanelli MG, Galavotti R, Martinelli N, Girelli D, et al. Detection of a large deletion in the P-selectin (SELP) gene. Mol Cell Probes. 2010;24(3):161-5.

58. Green D, Foiles N, Chan C, Kang J, Schreiner PJ, Liu K. An association between clotting factor VII and carotid intima-media thickness: the CARDIA study. Stroke. 2010;41(7):1417-22.

59. Ross TD, Coon BG, Yun S, Baeyens N, Tanaka K, Ouyang M, et al. Integrins in mechanotransduction. Curr Opin Cell Biol. 2013;25(5):613-8.

60. Mulvihill NT, Foley JB, Crean P, Walsh M. Prediction of cardiovascular risk using soluble cell adhesion molecules. Eur Heart J. 2002;23(20):1569-74.

61. Blann AD, Steele C, McCollum CN. The influence of smoking on soluble adhesion molecules and endothelial cell markers. Thrombosis Research. 1997;85(5):433-8.

62. DeSouza CA, Dengel DR, Macko RF, Cox K, Seals DR. Elevated levels of circulating cell adhesion molecules in uncomplicated essential hypertension. American Journal of Hypertension. 1997;10(12):1335-41.

63. Calabresi L, Gomaraschi M, Villa B, Omoboni L, Dmitrieff C, Franceschini G. Elevated soluble cellular adhesion molecules in subjects with low HDL-cholesterol. Arteriosclerosis, thrombosis, and vascular biology. 2002;22(4):656-61.

64. Hackman A, Abe Y, Insull Jr W, Pownall H, Smith L, Dunn K, et al. Levels of soluble cell adhesion molecules in patients with dyslipidemia. Circulation. 1996;93(7):1334-8.

65. Abe Y, El-Masri B, Kimball KT, Pownall H, Reilly CF, Osmundsen K, et al. Soluble cell adhesion molecules in hypertriglyceridemia and potential significance on monocyte adhesion. Arteriosclerosis, thrombosis, and vascular biology. 1998;18(5):723-31.

66. Rohde LE, Lee RT, Rivero J, Jamacochian M, Arroyo LH, Briggs W, et al. Circulating cell adhesion molecules are correlated with ultrasound-based assessment of carotid atherosclerosis. Arteriosclerosis, thrombosis, and vascular biology. 1998;18(11):1765-70.

67. Tanne D, Haim M, Boyko V, Goldbourt U, Reshef T, Matetzky S, et al. Soluble intercellular adhesion molecule-1 and risk of future ischemic stroke: a nested case-control study from the Bezafibrate Infarction Prevention (BIP) study cohort. Stroke. 2002;33(9):2182-6.

68. Ridker PM, Buring JE, Rifai N. Soluble P-selectin and the risk of future cardiovascular events. Circulation. 2001;103(4):491-5.

69. Belch J, Shaw J, Kirk G, McLaren M, Robb R, Maple C, et al. The white blood cell adhesion molecule E-selectin predicts restenosis in patients with intermittent claudication undergoing percutaneous transluminal angioplasty. Circulation. 1997;95(8):2027-31.

70. Moore KJ, Tabas I. Macrophages in the pathogenesis of atherosclerosis. Cell. 2011;145(3):341-55.

71. Park I, Kassiteridi C, Monaco C. Functional diversity of macrophages in vascular biology and disease. Vascul Pharmacol. 2017;99:13-22.

72. Serbina NV, Pamer EG. Monocyte emigration from bone marrow during bacterial infection requires signals mediated by chemokine receptor CCR2. Nat Immunol. 2006;7(3):311-7.

73. Robbins CS, Chudnovskiy A, Rauch PJ, Figueiredo JL, Iwamoto Y, Gorbatov R, et al. Extramedullary hematopoiesis generates Ly-6C(high) monocytes that infiltrate atherosclerotic lesions. Circulation. 2012;125(2):364-74.

74. Chinetti-Gbaguidi G, Colin S, Staels B. Macrophage subsets in atherosclerosis. Nat Rev Cardiol. 2015;12(1):10-7.

75. Gordon S, Martinez FO. Alternative activation of macrophages: mechanism and functions. Immunity. 2010;32(5):593-604.

76. Verreck FA, de Boer T, Langenberg DM, Hoeve MA, Kramer M, Vaisberg E, et al. Human IL-23-producing type 1 macrophages promote but IL-10-producing type 2 macrophages subvert immunity to (myco)bacteria. Proc Natl Acad Sci U S A. 2004;101(13):4560-5.

77. Mosser DM. The many faces of macrophage activation. J Leukoc Biol. 2003;73(2):209-12.

78. Kotwal GJ, Chien S. Macrophage Differentiation in Normal and Accelerated Wound Healing. Results Probl Cell Differ. 2017;62:353-64.

79. Khallou-Laschet J, Varthaman A, Fornasa G, Compain C, Gaston AT, Clement M, et al. Macrophage plasticity in experimental atherosclerosis. PLoS One. 2010;5(1):e8852.

80. Kadl A, Meher AK, Sharma PR, Lee MY, Doran AC, Johnstone SR, et al. Identification of a novel macrophage phenotype that develops in response to atherogenic phospholipids via Nrf2. Circ Res. 2010;107(6):737-46.

81. Wolfs IM, Stöger JL, Goossens P, Pöttgens C, Gijbels MJ, Wijnands E, et al. Reprogramming macrophages to an anti-inflammatory phenotype by helminth antigens reduces murine atherosclerosis. Faseb j. 2014;28(1):288-99.

82. Harmon EY, Fronhofer V, 3rd, Keller RS, Feustel PJ, Zhu X, Xu H, et al. Anti-inflammatory immune skewing is atheroprotective: Apoe−/−FcγRIIb−/− mice develop fibrous carotid plaques. J Am Heart Assoc. 2014;3(6):e001232.

83. George J, Shoenfeld Y, Gilburd B, Afek A, Shaish A, Harats D. Requisite role for interleukin-4 in the acceleration of fatty streaks induced by heat shock protein 65 or Mycobacterium tuberculosis. Circ Res. 2000;86(12):1203-10.

84. Choi JH, Do Y, Cheong C, Koh H, Boscardin SB, Oh YS, et al. Identification of antigen-presenting dendritic cells in mouse aorta and cardiac valves. J Exp Med. 2009;206(3):497-505.

85. Jongstra-Bilen J, Haidari M, Zhu SN, Chen M, Guha D, Cybulsky MI. Low-grade chronic inflammation in regions of the normal mouse arterial intima predisposed to atherosclerosis. J Exp Med. 2006;203(9):2073-83.

86. Choi JH, Cheong C, Dandamudi DB, Park CG, Rodriguez A, Mehandru S, et al. Flt3 signaling-dependent dendritic cells protect against atherosclerosis. Immunity. 2011;35(5):819-31.

87. Persson EK, Uronen-Hansson H, Semmrich M, Rivollier A, Hägerbrand K, Marsal J, et al. IRF4 transcription-factor-dependent CD103(+)CD11b(+) dendritic cells drive mucosal T helper 17 cell differentiation. Immunity. 2013;38(5):958-69.

88. Schlitzer A, McGovern N, Teo P, Zelante T, Atarashi K, Low D, et al. IRF4 transcription factor-dependent CD11b+ dendritic cells in human and mouse control mucosal IL-17 cytokine responses. Immunity. 2013;38(5):970-83.

89. Busch M, Westhofen TC, Koch M, Lutz MB, Zernecke A. Dendritic cell subset distributions in the aorta in healthy and atherosclerotic mice. PLoS One. 2014;9(2):e88452.

90. Friedman GD, Klatsky AL, Siegelaub AB. The leukocyte count as a predictor of myocardial infarction. N Engl J Med. 1974;290(23):1275-8.

91. Guasti L, Dentali F, Castiglioni L, Maroni L, Marino F, Squizzato A, et al. Neutrophils and clinical outcomes in patients with acute coronary syndromes and/or cardiac revascularisation. A systematic review on more than 34,000 subjects. Thromb Haemost. 2011;106(4):591-9.

92. Drechsler M, Megens RT, van Zandvoort M, Weber C, Soehnlein O. Hyperlipidemia-triggered neutrophilia promotes early atherosclerosis. Circulation. 2010;122(18):1837-45.

93. Silvestre-Roig C, Braster Q, Ortega-Gomez A, Soehnlein O. Neutrophils as regulators of cardiovascular inflammation. Nat Rev Cardiol. 2020;17(6):327-40.

94. Steinman RM. Decisions about dendritic cells: past, present, and future. Annu Rev Immunol. 2012;30:1-22.

95. Veerman KM, Carlow DA, Shanina I, Priatel JJ, Horwitz MS, Ziltener HJ. PSGL-1 regulates the migration and proliferation of CD8(+) T cells under homeostatic conditions. J Immunol. 2012;188(4):1638-46.

96. Erbel C, Sato K, Meyer FB, Kopecky SL, Frye RL, Goronzy JJ, et al. Functional profile of activated dendritic cells in unstable atherosclerotic plaque. Basic Res Cardiol. 2007;102(2):123-32.

97. Buono C, Binder CJ, Stavrakis G, Witztum JL, Glimcher LH, Lichtman AH. T-bet deficiency reduces atherosclerosis and alters plaque antigen-specific immune responses. Proc Natl Acad Sci U S A. 2005;102(5):1596-601.

98. Frostegård J, Ulfgren AK, Nyberg P, Hedin U, Swedenborg J, Andersson U, et al. Cytokine expression in advanced human atherosclerotic plaques: dominance of pro-inflammatory (Th1) and macrophage-stimulating cytokines. Atherosclerosis. 1999;145(1):33-43.

99. Saigusa R, Winkels H, Ley K. T cell subsets and functions in atherosclerosis. Nat Rev Cardiol. 2020;17(7):387-401.

100. Wolf D, Ley K. Immunity and Inflammation in Atherosclerosis. Circ Res. 2019;124(2):315-27.

101. Amento EP, Ehsani N, Palmer H, Libby P. Cytokines and growth factors positively and negatively regulate interstitial collagen gene expression in human vascular smooth muscle cells. Arterioscler Thromb. 1991;11(5):1223-30.

102. Orecchioni M, Ghosheh Y, Pramod AB, Ley K. Macrophage Polarization: Different Gene Signatures in M1(LPS+) vs. Classically and M2(LPS-) vs. Alternatively Activated Macrophages. Front Immunol. 2019;10:1084.

103. Rocha VZ, Folco EJ, Sukhova G, Shimizu K, Gotsman I, Vernon AH, et al. Interferon-gamma, a Th1 cytokine, regulates fat inflammation: a role for adaptive immunity in obesity. Circ Res. 2008;103(5):467-76.

104. Davenport P, Tipping PG. The role of interleukin-4 and interleukin-12 in the progression of atherosclerosis in apolipoprotein E-deficient mice. Am J Pathol. 2003;163(3):1117-25.

105. Cardilo-Reis L, Gruber S, Schreier SM, Drechsler M, Papac-Milicevic N, Weber C, et al. Interleukin-13 protects from atherosclerosis and modulates plaque composition by skewing the macrophage phenotype. EMBO Mol Med. 2012;4(10):1072-86.

106. Sämpi M, Ukkola O, Päivänsalo M, Kesäniemi YA, Binder CJ, Hörkkö S. Plasma interleukin-5 levels are related to antibodies binding to oxidized low-density lipoprotein and to decreased subclinical atherosclerosis. J Am Coll Cardiol. 2008;52(17):1370-8.

107. Silveira A, McLeod O, Strawbridge RJ, Gertow K, Sennblad B, Baldassarre D, et al. Plasma IL-5 concentration and subclinical carotid atherosclerosis. Atherosclerosis. 2015;239(1):125-30.

108. Fontenot JD, Gavin MA, Rudensky AY. Pillars Article: Foxp3 Programs the Development and Function of CD4+CD25+ Regulatory T Cells. Nat. Immunol. 2003. 4: 330-336. J Immunol. 2017;198(3):986-92.

109. Freiberg BA, Kupfer H, Maslanik W, Delli J, Kappler J, Zaller DM, et al. Staging and resetting T cell activation in SMACs. Nat Immunol. 2002;3(10):911-7.

110. Moore KW, Vieira P, Fiorentino DF, Trounstine ML, Khan TA, Mosmann TR. Homology of cytokine synthesis inhibitory factor (IL-10) to the Epstein-Barr virus gene BCRFI. Science. 1990;248(4960):1230-4.

111. Spitz C, Winkels H, Bürger C, Weber C, Lutgens E, Hansson GK, et al. Regulatory T cells in atherosclerosis: critical immune regulatory function and therapeutic potential. Cell Mol Life Sci. 2016;73(5):901-22.

112. de Boer OJ, van der Meer JJ, Teeling P, van der Loos CM, van der Wal AC. Low numbers of FOXP3 positive regulatory T cells are present in all developmental stages of human atherosclerotic lesions. PLoS One. 2007;2(8):e779.

113. Heller EA, Liu E, Tager AM, Yuan Q, Lin AY, Ahluwalia N, et al. Chemokine CXCL10 promotes atherogenesis by modulating the local balance of effector and regulatory T cells. Circulation. 2006;113(19):2301-12.

114. Schäfer S, Zernecke A. CD8(+) T Cells in Atherosclerosis. Cells. 2020;10(1).

115. Kolbus D, Ramos OH, Berg KE, Persson J, Wigren M, Björkbacka H, et al. CD8+ T cell activation predominate early immune responses to hypercholesterolemia in Apoe^{-}(/)$^{-}$ mice. BMC Immunol. 2010;11:58.

116. Cochain C, Koch M, Chaudhari SM, Busch M, Pelisek J, Boon L, et al. CD8+ T Cells Regulate Monopoiesis and Circulating Ly6C-high Monocyte Levels in Atherosclerosis in Mice. Circ Res. 2015;117(3):244-53.

117. Getz GS, Reardon CA. Animal models of atherosclerosis. Arterioscler Thromb Vasc Biol. 2012;32(5):1104-15.

118. Meir KS, Leitersdorf E. Atherosclerosis in the apolipoprotein-E-deficient mouse: a decade of progress. Arterioscler Thromb Vasc Biol. 2004;24(6):1006-14.

119. Zhang SH, Reddick RL, Piedrahita JA, Maeda N. Spontaneous hypercholesterolemia and arterial lesions in mice lacking apolipoprotein E. Science. 1992;258(5081):468-71.

120. Ishibashi S, Brown MS, Goldstein JL, Gerard RD, Hammer RE, Herz J. Hypercholesterolemia in low density lipoprotein receptor knockout mice and its reversal by adenovirus-mediated gene delivery. J Clin Invest. 1993;92(2):883-93.

121. Ishibashi S, Goldstein JL, Brown MS, Herz J, Burns DK. Massive xanthomatosis and atherosclerosis in cholesterol-fed low density lipoprotein receptor-negative mice. J Clin Invest. 1994;93(5):1885-93.

122. Bjørklund MM, Hollensen AK, Hagensen MK, Dagnaes-Hansen F, Christoffersen C, Mikkelsen JG, et al. Induction of atherosclerosis in mice and hamsters without germline genetic engineering. Circ Res. 2014;114(11):1684-9.

123. Roche-Molina M, Sanz-Rosa D, Cruz FM, García-Prieto J, López S, Abia R, et al. Induction of sustained hypercholesterolemia by single adeno-associated virus-mediated gene transfer of mutant hPCSK9. Arterioscler Thromb Vasc Biol. 2015;35(1):50-9.

124. Oppi S, Lüscher TF, Stein S. Mouse Models for Atherosclerosis Research-Which Is My Line? Front Cardiovasc Med. 2019;6:46.

125. Mahley RW. Apolipoprotein E: cholesterol transport protein with expanding role in cell biology. Science. 1988;240(4852):622-30.

126. Sehayek E, Shefer S, Nguyen LB, Ono JG, Merkel M, Breslow JL. Apolipoprotein E regulates dietary cholesterol absorption and biliary cholesterol excretion: studies in C57BL/6 apolipoprotein E knockout mice. Proc Natl Acad Sci U S A. 2000;97(7):3433-7.

127. Jawień J, Nastałek P, Korbut R. Mouse models of experimental atherosclerosis. J Physiol Pharmacol. 2004;55(3):503-17.

128. Nakashima Y, Plump AS, Raines EW, Breslow JL, Ross R. ApoE-deficient mice develop lesions of all phases of atherosclerosis throughout the arterial tree. Arterioscler Thromb. 1994;14(1):133-40.

129. Emini Veseli B, Perrotta P, De Meyer GRA, Roth L, Van der Donckt C, Martinet W, et al. Animal models of atherosclerosis. Eur J Pharmacol. 2017;816:3-13.

130. Fullerton SM, Shirman GA, Strittmatter WJ, Matthew WD. Impairment of the blood-nerve and blood-brain barriers in apolipoprotein e knockout mice. Exp Neurol. 2001;169(1):13-22.

131. Gutman CR, Strittmatter WJ, Weisgraber KH, Matthew WD. Apolipoprotein E binds to and potentiates the biological activity of ciliary neurotrophic factor. J Neurosci. 1997;17(16):6114-21.

132. Holtzman DM, Pitas RE, Kilbridge J, Nathan B, Mahley RW, Bu G, et al. Low density lipoprotein receptor-related protein mediates apolipoprotein E-dependent neurite outgrowth in a central nervous system-derived neuronal cell line. Proc Natl Acad Sci U S A. 1995;92(21):9480-4.

133. Huang DY, Weisgraber KH, Strittmatter WJ, Matthew WD. Interaction of apolipoprotein E with laminin increases neuronal adhesion and alters neurite morphology. Exp Neurol. 1995;136(2):251-7.

134. Laskowitz DT, Goel S, Bennett ER, Matthew WD. Apolipoprotein E suppresses glial cell secretion of TNF alpha. J Neuroimmunol. 1997;76(1-2):70-4.

135. Laskowitz DT, Matthew WD, Bennett ER, Schmechel D, Herbstreith MH, Goel S, et al. Endogenous apolipoprotein E suppresses LPS-stimulated microglial nitric oxide production. Neuroreport. 1998;9(4):615-8.

136. Nishitsuji K, Hosono T, Nakamura T, Bu G, Michikawa M. Apolipoprotein E Regulates the Integrity of Tight Junctions in an Isoform-dependent Manner in an in Vitro Blood-Brain Barrier Model*. Journal of Biological Chemistry. 2011;286(20):17536-42.

137. Bell RD, Winkler EA, Singh I, Sagare AP, Deane R, Wu Z, et al. Apolipoprotein E controls cerebrovascular integrity via cyclophilin A. Nature. 2012;485(7399):512-6.

138. Alata W, Ye Y, St-Amour I, Vandal M, Calon F. Human apolipoprotein E ε4 expression impairs cerebral vascularization and blood-brain barrier function in mice. J Cereb Blood Flow Metab. 2015;35(1):86-94.

139. Poirier J, Miron J, Picard C, Gormley P, Théroux L, Breitner J, et al. Apolipoprotein E and lipid homeostasis in the etiology and treatment of sporadic Alzheimer's disease. Neurobiol Aging. 2014;35 Suppl 2(Suppl 2):S3-10.

140. Plump AS, Smith JD, Hayek T, Aalto-Setälä K, Walsh A, Verstuyft JG, et al. Severe hypercholesterolemia and atherosclerosis in apolipoprotein E-deficient mice created by homologous recombination in ES cells. Cell. 1992;71(2):343-53.

141. Lo Sasso G, Schlage WK, Boué S, Veljkovic E, Peitsch MC, Hoeng J. The Apoe(-/-) mouse model: a suitable model to study cardiovascular and respiratory diseases in the context of cigarette smoke exposure and harm reduction. J Transl Med. 2016;14(1):146.

142. Getz GS, Reardon CA. PCSK9 and lipid metabolism and atherosclerosis: animal models. Vessel Plus. 2021;5:17.

143. Cunningham D, Danley DE, Geoghegan KF, Griffor MC, Hawkins JL, Subashi TA, et al. Structural and biophysical studies of PCSK9 and its mutants linked to familial hypercholesterolemia. Nature structural & molecular biology. 2007;14(5):413-9.

144. Abifadel M, Varret M, Rabès J-P, Allard D, Ouguerram K, Devillers M, et al. Mutations in PCSK9 cause autosomal dominant hypercholesterolemia. Nature genetics. 2003;34(2):154-6.

145. Al-Mashhadi RH, Sørensen CB, Kragh PM, Christoffersen C, Mortensen MB, Tolbod LP, et al. Familial hypercholesterolemia and atherosclerosis in cloned minipigs created by DNA transposition of a human PCSK9 gain-of-function mutant. Science translational medicine. 2013;5(166):166ra1-ra1.

146. Kourimate S, Chétiveaux M, Jarnoux AL, Lalanne F, Costet P. Cellular and secreted pro-protein convertase subtilisin/kexin type 9 catalytic activity in hepatocytes. Atherosclerosis. 2009;206(1):134-40.

147. Cerrone M, Noorman M, Lin X, Chkourko H, Liang F-X, Van Der Nagel R, et al. Sodium current deficit and arrhythmogenesis in a murine model of plakophilin-2 haploinsufficiency. Cardiovascular research. 2012;95(4):460-8.

148. Kaspar BK, Roth DM, Chin Lai N, Drumm JD, Erickson DA, McKirnan MD, et al. Myocardial gene transfer and long-term expression following intracoronary delivery of adeno-associated virus. The Journal of Gene Medicine: A cross-disciplinary journal for research on the science of gene transfer and its clinical applications. 2005;7(3):316-24.

149. Suhy DA, Kao S-C, Mao T, Whiteley L, Denise H, Souberbielle B, et al. Safe, long-term hepatic expression of anti-HCV shRNA in a nonhuman primate model. Molecular Therapy. 2012;20(9):1737-49.

150. Goettsch C, Hutcheson JD, Hagita S, Rogers MA, Creager MD, Pham T, et al. A single injection of gain-of-function mutant PCSK9 adeno-associated virus vector induces cardiovascular calcification in mice with no genetic modification. Atherosclerosis. 2016;251:109-18.

151. Ezzati M, Henley SJ, Thun MJ, Lopez AD. Role of smoking in global and regional cardiovascular mortality. Circulation. 2005;112(4):489-97.

152. Shahandeh N, Chowdhary H, Middlekauff HR. Vaping and cardiac disease. Heart. 2021;107(19):1530-5.

153. Muthumalage T, Prinz M, Ansah KO, Gerloff J, Sundar IK, Rahman I. Inflammatory and oxidative responses induced by exposure to commonly used e-cigarette flavoring chemicals and flavored e-liquids without nicotine. Frontiers in physiology. 2018:1130.

154. Zhao D, Aravindakshan A, Hilpert M, Olmedo P, Rule AM, Navas-Acien A, et al. Metal/metalloid levels in electronic cigarette liquids, aerosols, and human biosamples: a systematic review. Environmental health perspectives. 2020;128(3):036001.

155. Vindhyal MR, Ndunda P, Munguti C, Vindhyal S, Okut H. Impact on cardiovascular outcomes among e-cigarette users: a review from National Health Interview Surveys. Journal of the American College of Cardiology. 2019;73(9S2):11-.

156. Espinoza-Derout J, Hasan KM, Shao XM, Jordan MC, Sims C, Lee DL, et al. Chronic intermittent electronic cigarette exposure induces cardiac dysfunction and atherosclerosis in apolipoprotein-E knockout mice. American Journal of Physiology-Heart and Circulatory Physiology. 2019;317(2):H445-H59.

157. Szostak J, Wong ET, Titz B, Lee T, Wong SK, Low T, et al. A 6-month systems toxicology inhalation study in ApoE−/− mice demonstrates reduced cardiovascular effects of E-vapor aerosols compared with cigarette smoke. American Journal of Physiology-Heart and Circulatory Physiology. 2020;318(3):H604-H31.

158. Vogel EA, Prochaska JJ, Ramo DE, Andres J, Rubinstein ML. Adolescents' E-Cigarette Use: Increases in Frequency, Dependence, and Nicotine Exposure Over 12 Months. J Adolesc Health. 2019;64(6):770-5.

159. Leavens ELS, Stevens EM, Brett EI, Hébert ET, Villanti AC, Pearson JL, et al. JUUL electronic cigarette use patterns, other tobacco product use, and reasons for use among ever users: Results from a convenience sample. Addict Behav. 2019;95:178-83.

160. Maxwell KN, Breslow JL. Adenoviral-mediated expression of Pcsk9 in mice results in a low-density lipoprotein receptor knockout phenotype. Proc Natl Acad Sci U S A. 2004;101(18):7100-5.

161. Miller M. Dyslipidemia and cardiovascular risk: the importance of early prevention. QJM: An International Journal of Medicine. 2009;102(9):657-67.

162. Lee HW, Park SH, Weng MW, Wang HT, Huang WC, Lepor H, et al. E-cigarette smoke damages DNA and reduces repair activity in mouse lung, heart, and bladder as well as in human lung and bladder cells. Proc Natl Acad Sci U S A. 2018;115(7):E1560-e9.

163. Corriden R, Moshensky A, Bojanowski CM, Meier A, Chien J, Nelson RK, et al. E-cigarette use increases susceptibility to bacterial infection by impairment of human neutrophil chemotaxis, phagocytosis, and NET formation. Am J Physiol Cell Physiol. 2020;318(1):C205-c14.

164. Hwang JH, Lyes M, Sladewski K, Enany S, McEachern E, Mathew DP, et al. Electronic cigarette inhalation alters innate immunity and airway cytokines while increasing the virulence of colonizing bacteria. J Mol Med (Berl). 2016;94(6):667-79.

165. Petersen D, Norris K, Thompson J. A comparative study of the disposition of nicotine and its metabolites in three inbred strains of mice. Drug Metabolism and Disposition. 1984;12(6):725-31.

166. Nardone N, Helen GS, Addo N, Meighan S, Benowitz NL. JUUL electronic cigarettes: nicotine exposure and the user experience. Drug and alcohol dependence. 2019;203:83-7.

167. St Helen G, Novalen M, Heitjan DF, Dempsey D, Jacob P, Aziziyeh A, et al. Reproducibility of the Nicotine Metabolite Ratio in Cigarette SmokersNMR Reproducibility and Stability. Cancer epidemiology, biomarkers & prevention. 2012;21(7):1105-14.

168. Linton MF, Yancey PG, Davies SS, Jerome WG, Linton EF, Song WL, et al. The Role of Lipids and Lipoproteins in Atherosclerosis. In: Feingold KR, Anawalt B, Boyce A, Chrousos G, de Herder WW, Dhatariya K, et al., editors. Endotext. South Dartmouth (MA): MDText.com, Inc.

169. Ortiz-Muñoz G, Houard X, Martín-Ventura JL, Ishida BY, Loyau S, Rossignol P, et al. HDL antielastase activity prevents smooth muscle cell anoikis, a potential new antiatherogenic property. Faseb j. 2009;23(9):3129-39.

170. Janzon L, Berntorp K, Hanson M, Lindell SE, Trell E. Glucose tolerance and smoking: a population study of oral and intravenous glucose tolerance tests in middle-aged men. Diabetologia. 1983;25(2):86-8.

171. Zhang Z, Jiao Z, Blaha MJ, Osei A, Sidhaye V, Ramanathan M, Jr., et al. The Association Between E-Cigarette Use and Prediabetes: Results From the Behavioral Risk Factor Surveillance System, 2016-2018. Am J Prev Med. 2022;62(6):872-7.

172. Shi H, Fan X, Horton A, Haller ST, Kennedy DJ, Schiefer IT, et al. The effect of electronic-cigarette vaping on cardiac function and angiogenesis in mice. Scientific reports. 2019;9(1):1-9.

173. Ninomiya Y, Shigemura N, Yasumatsu K, Ohta R, Sugimoto K, Nakashima K, et al. Leptin and sweet taste. 2002.

174. Peters JM, Shah YM, Gonzalez FJ. The role of peroxisome proliferator-activated receptors in carcinogenesis and chemoprevention. Nature Reviews Cancer. 2012;12(3):181-95.

175. Bronte V, Pittet MJ. The spleen in local and systemic regulation of immunity. Immunity. 2013;39(5):806-18.

176. Ford WLW. The traffic of lymphocytes. Seminars in hematology.6(1):67-83.

177. Zhu J, Paul WE. CD4 T cells: fates, functions, and faults. Blood. 2008;112(5):1557-69.

178. Marits P, Wikström AC, Popadic D, Winqvist O, Thunberg S. Evaluation of T and B lymphocyte function in clinical practice using a flow cytometry based proliferation assay. Clin Immunol. 2014;153(2):332-42.

179. Angel S, von Briesen H, Oh Y-J, Baller MK, Zimmermann H, Germann A. Toward optimal cryopreservation and storage for achievement of high cell recovery and maintenance of cell viability and T cell functionality. Biopreservation and biobanking. 2016;14(6):539-47.

180. Audrain-McGovern J, Benowitz NL. Cigarette smoking, nicotine, and body weight. Clin Pharmacol Ther. 2011;90(1):164-8.

181. Lempert LK, Halpern-Felsher B. The E-Cigarette Phenomenon: What it is, Why it is Happening, and What You Should Know About it. In: Walley SC, Wilson K, editors. Electronic Cigarettes and Vape Devices : A Comprehensive Guide for Clinicians and Health Professionals. Cham: Springer International Publishing; 2021. p. 17-36.

182. Do EK, O'Connor K, Perks SN, Soule EK, Eissenberg T, Amato MS, et al. E-cigarette device and liquid characteristics and E-cigarette dependence: A pilot study of pod-based and disposable E-cigarette users. Addictive Behaviors. 2022;124:107117.